Energy Reports 8 (2022) 10244–10271

Contents lists available at ScienceDirect

Energy Reports

journal homepage: www.elsevier.com/locate/egyr

Research paper

Energy flexibility and viability enhancement for an ocean-energy-supported zero-emission office building with respect to both existing and advanced utility business models with dynamic responsive incentives

Shijie Zhou [a], Sunliang Cao [a,b,c,*]

[a] Renewable Energy Research Group (RERG), Department of Building Environment and Energy Engineering, Faculty of Construction and Environment, The Hong Kong Polytechnic University, Kowloon, Hong Kong Special Administrative Region
[b] Research Institute for Sustainable Urban Development (RISUD), The Hong Kong Polytechnic University, Kowloon, Hong Kong Special Administrative Region
[c] Research Institute for Smart Energy (RISE), The Hong Kong Polytechnic University, Kowloon, Hong Kong Special Administrative Region

ARTICLE INFO

Article history:
Received 18 May 2022
Received in revised form 15 July 2022
Accepted 2 August 2022
Available online 18 August 2022

Keywords:
Energy flexibility control
Floating photovoltaic panel system (FPV)
Peak demand management (PDM)
Tidal stream generator (TSG)
Zero-emission building (ZEB)

ABSTRACT

The foreseeable large-scale deployment of intermittent renewable energy systems in the future and fluctuations in energy markets can severely affect the operation and stability of smart grids, creating significant uncertainty and instability in the electricity supply and demand. It is believed that the mismatch between energy demand of a building and instantaneous renewable energy generation can be reduced by controlling energy use through the energy flexibility of the respective building. Enhancing the energy flexibility of a zero-emission building can satisfy the demands of the energy network around the building and contribute to the resilience of the energy system. Meanwhile, in an electricity tariff model with a distinction between peak and off-peak periods, enhancing energy flexibility in buildings can reduce the operating costs of electricity consumption, with benefits to the economic performance of the building itself. In this study, a simulated hypothetical zero-emission office building near the coast with a floating photovoltaic system and tidal stream generator system in Hong Kong from previous study were used in a case study to investigate the impact of energy flexibility control with stationary batteries as the source of energy flexibility. Two flexibility control strategies were designed to demonstrate their impact on the economic performance of the system. After incorporating the "Peak Demand Management" (PDM) programme in Hong Kong, variations in the economic performance of the system were demonstrated through simulations. Considering the incentive provided by the PDM programme, the possibility of achieving a neutral economic performance at different percentages of renewable energy generation over a 20-year life cycle without the feed-in tariff was investigated. Furthermore, two possible modifications for business models and the PDM programme are proposed. The simulation results indicate that both suggestions can significantly improve the economic performance of the system.

1. Introduction and background

1.1. Background

The development of renewable energy sources is gradually gaining interest worldwide owing to the continuous increase in energy demand and the negative impact of traditional fossil energy sources on the environment. Carbon neutrality was one of the popular topics discussed among countries at the 2021 G20 Rome summit to further reduce the impact of fossil energy (CNBC, 2021). This makes zero-energy or zero-emission buildings a very important concept; zero-emission buildings are often accompanied by renewable energy generation systems of various scales. However, the foreseeable large-scale deployment of intermittent renewable energy systems in the future and fluctuations in the energy market could severely affect the operation and stability of smart grids and create significant uncertainty and instability in the electricity supply and demand. Therefore, International

* Corresponding author at: Renewable Energy Research Group (RERG), Department of Building Environment and Energy Engineering, Faculty of Construction and Environment, The Hong Kong Polytechnic University, Kowloon, Hong Kong Special Administrative Region.
E-mail addresses: sunliang.cao@polyu.edu.hk, caosunliang@msn.com (S. Cao).

https://doi.org/10.1016/j.egyr.2022.08.005

Acronym

AHU	Air handling unit
AC	Air handling unit cooling
BIPV	Building integrated photovoltaic system
B_t	Benefit of the period t
C_t	Cost of the period t
DHW	Domestic hot water
ED	Energy demand
FPV	Floating photovoltaic
FC1	Flexibility Control 1
FC2	Flexibility Control 2
$G_{RE:}$	Renewable energy generation
HX	Heat exchanger
i	Interest rate
NPV_{rel}	Relative net present value
PDM	Peak Demand Management programme
PSI_{peak}	Peak shaving indicator
REe	Renewable electricity
SC	Space cooling
S1	Scenario 1: All-grid case
S2	Scenario 2: Zero-emission case, battery interacts with the grid
S3	Scenario 3: Zero-emission case, battery interacts with the grid and renewable energy
TSG	Tidal stream generator
$VFI_{offpeak}$	Off-peak valley filling indicator
ZEB	Zero-emission/energy building

Energy Agency (IEA) academics believe that it is necessary to control energy use to ensure consistency with instantaneous energy generation. Energy flexibility, the ability to manage demand based on the local climate, user requirements, and energy network requirements, through the building itself is an attractive method of controlling energy use as it does not require additional infrastructure. Enhancing the energy flexibility in buildings can relieve pressure on the electricity grid during peak periods and contribute to the resilience of future energy systems (IEA, 2021). Owing to the unstable output of current renewable energy generation systems, a significant mismatch often occurs between energy demand and renewable energy generation in zero-energy buildings. Smart grids were developed to solve the power grid challenges including energy reliability, safety and security, the operation and stability of smart grids and its Advanced metring infrastructures can help the energy flexibility control and the demand response of the consumers (Ghasempour, 2017). The investigation of flexibility enhancement in zero-energy buildings can reduce this mismatch, increase the self-consumption of renewable energy throughout the system, and reduce pressure on the grid during peak periods. Therefore, further research on this topic is significant.

1.2. Literature review

In the academic field, in addition to existing renewable energy sources, ocean or ocean-related renewable energy is becoming increasingly popular because of its significant potential. Ocean thermal energy is typically studied in combination with air-conditioning systems of buildings near the coast to reduce energy consumption. Elahee and Jugoo investigated the engineering, economic, and environmental impacts of an air-conditioning system using cold seawater in a data centre that operates throughout the day. The energy demand can be 94% lower than that of traditional cooling systems (Elahee and Jugoo, 2013). Mokhtari and Arabkoohsar conducted a feasibility study of seawater cooling systems for data centres and developed a thermodynamic model to determine their optimal size and operating conditions. Compared with conventional cooling systems, a seawater cooling system with a water inlet at a depth of 700 m below in the Caspian Sea can save 78% of energy consumption (Mokhtari and Arabkoohsar, 2021). The research and application of floating photovoltaics (FPVs) on the sea surface are also being conducted to reduce land use. Cazzaniga and Rosa-Clot analysed the current growing development of FPV systems and forecast trends to 2030. They concluded that FPV-installed power will double every year because of the minimised use of occupied land resources (Cazzaniga and Rosa-Clot, 2021). Coles et al. quantified the technical, economic, and environmental performances of hybrid systems with tidal stream turbines and battery storage to replace oil generators. The tidal stream system reduces 78% of carbon emissions (Coles et al., 2021). Guo et al. explored the techno-economic-environmental feasibility of an integrated zero-energy hotel building with zero-emission electric boats supported by a hybrid FPV and wave-energy converter renewable energy system (Guo et al., 2021). Luo et al. evaluated the techno-economic feasibility of a coastal zero-energy hotel building supported by wave energy converters and offshore wind turbines (Luo et al., 2022). Soliman et al. provided a new energy management control technique for a smart microgrid using batteries, wind energy, solar energy, and tidal energy sources. This new control technique can improve the energy output from hybrid renewable energy sources and ensure smooth output power (Soliman et al., 2021). Park and Lee reviewed a case study on tidal power in South Korea. The Shihwa Tidal Power Plant, the subject of their study, is both an advanced energy generation plant and an eco-friendly means to resurrect a 'dead lake' by circulating the water of the lake (Park and Lee, 2021). Chiang and Young introduced an engineering project for a flood-detention pond surface-type FPV power generation system to improve the sustainable use of photovoltaic (PV) power generation and economic performance (Chiang and Young, 2022).

Meanwhile, owing to the continued development of renewable energy and the integration of different sources, flexibility control of the demand side is required for grid management and to improve the self-consumption of renewable energy (Finck et al., 2018). Many researchers have focused on the possible source of energy flexibility within zero-energy buildings to enhance their techno-economic performance. Finck et al. studied optimal control using a heat pump, electric heaters, and thermal energy storage tanks to improve the demand flexibility of an office building. Different performance indicators were used to quantify flexibility. A simulation case study indicated that an integrated building heating system with a water tank, phase change material tank, and thermochemical material tank can improve flexibility with optimal control (Finck et al., 2018). Liu and Herselberg studied a nearly zero-energy building with weather predictive controls. The energy flexibility performances of different control strategies for cooling systems were investigated and compared. Their results indicated that approximately 80% of the energy consumption during the high-price period could be removed using suitable control methods (Liu and Heiselberg, 2019). Lu et al. investigated the energy flexibility of cooling systems with building thermal mass in near-zero energy buildings evaluated using a simulation-based strategy, including control and quantification methods. The results indicated that the peak power and peak energy can be reduced by more than 50% in the

targeted building (Lu et al., 2021). Salpakari and Lund proposed a model that combines a heat pump with storage, a battery, and shiftable appliances to balance the mismatch between electricity production from on-site PV systems and building demand. Based on a case study of an actual low-energy house in Finland, compared with inflexible control, the cost-optimal control of the aforementioned model can save approximately 20% of the annual electricity bill (Salpakari and Lund, 2016). Dar et al. analysed two configurations of heat pumps with thermal energy storage and four control strategies to investigate the flexibility performance of net-zero-energy buildings. The performance indicated that the electricity bill can be reduced and the building self-consumption of renewable energy can be improved with a proper control strategy (Dar et al., 2014). Zhou and Cao presented a model combining building-integrated and vehicle-integrated PVs. The energy flexibility performance of the hybrid building–vehicle system was assessed, grid-responsive energy control strategies were proposed, and techno-economic feasibility was discussed (Zhou and Cao, 2019). Selvakkumaran et al. reviewed 15 scientific articles on business models for prosumers in the district energy grid in terms of their flexibility (Selvakkumaran et al., 2021).

Regarding the increasing pressure on electricity grids during peak periods, various countries and regions have their own demand response or demand-side management programmes, and research on these programmes is gradually increasing. Javaid et al. presented a home-energy-management control system that can schedule single or multiple home appliances integrated with renewable energy sources to adjust the household energy load and participate in demand-side management. A simulation demonstrated that their proposed scheme can reduce the electricity bill by up to 48% (Javaid et al., 2018). Anzar et al. investigated the feasibility of a home-energy-management system integrated with renewable energy resources for effective demand-side management in a smart grid based on a simulation. Their results indicated the effectiveness of this approach (Anzar et al., 2017). Irshad et al. proposed a user-friendly technique using a genetic algorithm to schedule residential loads in a smart grid and overcome user inconvenience. A renewable energy source was used to satisfy the peak-hour demand and improve load scheduling. Simulation results indicated that this algorithm was effective in scheduling the load and reducing the peak-to-average load ratio (Irshad et al., 2020). Huang et al. reviewed the fundamental theory, framework design, and potential of demand response based on the traditional demand response, and evaluated the current research and application of an integrated demand response with multi-energy systems such as electricity, heat, natural gas, and other energy sources (Huang et al., 2019). Kirkerud et al. believed that flexibility can be improved in renewable-based energy systems by increasing the demand response from households, the industry, and the tertiary sector. They studied the future economic potential demand response in the northern European region and concluded that demand response may contribute to peak shaving of up to 18.6% of the total peak load in 2050 (Kirkerud et al., 2021). Faria and Vale proposed a methodology for activating or deactivating different demand response programs during an event to cover deviations from the target (Faria and Vale, 2022). Tostado-Véliz et al. developed a home energy management system that included three effective demand response strategies. Their results indicated that the indicators of different goals from demand response programs can be improved by 70%, while the electricity bill was only slightly increased (Tostado-Véliz et al., 2022).

Research on smart grids is also a key focus for energy flexibility control. Ghasempour mentioned that smart grid has been designed to address the challenges of the grid including reliability, safety, economics and energy security. He introduced one of the major functions of the smart grid: the Advanced metring infrastructure (AMI) and described the general requirements and challenges of a communication infrastructure. The proposition of different networks and technologies are also investigated for AMI, including the scalability of different AMI architectures and a scalable hybrid AMI architecture (Ghasempour, 2017). Lou proposed a new solution based on Web Service Mining in smart grid infrastructures to reduce the response time and services request. This solution establishes an automatic method to integrate and take advantage of modern and old systems in the same infrastructure without investment in the adaptation. They also present a smart grid architecture with a hierarchical, distributed, and autonomous structure to address the challenge of smart distribution grids based on a smart city project (Lou, 2017). Ghasempour reviewed and summarised that smart grid is one of the most important applications of Internet of Things (IoT), and discussed IoT, smart grid and their connections, as well as the IoT architectures, requirements for using IoT, applications and services in smart grid (Ghasempour, 2019). In another of his research, he proposed an aggregation-based indirect architecture for advanced metring infrastructure architecture in help smart grid. A power consumption model was developed for each regional aggregator (RA) and neighbourhood area network (NAN) lifetime based on the model was defined. The simulation results verified the model can balanced the cost of RAs and NAN lifetime (Ghasempour, 2016). Bhattacharya et al. studied the incentive mechanisms for smart grid to encourage active and voluntary participation from consumers through the production of renewable energy. They reviewed the start-of-the-art contributions of incentive mechanisms in smart grids and discussed multiple technologies used to implement incentive mechanisms. The challenges and open issues related to such incentive mechanisms were also identified (Bhattacharya et al., 2022).

1.3. Scientific gaps and novelties

Based on the aforementioned literature review, several scientific gaps can be observed, as summarised below.

First, most of the current research on ocean energy is focused on improving and enhancing the performance and efficiency of technologies associated with the application of different ocean or ocean-related energy resources to better utilise these resources and the impact of these technologies. Few studies have focused on the use of seawater cooling systems to reduce the energy consumption of buildings. Moreover, few researchers have integrated different ocean energy sources to achieve the goal of zero-energy buildings and verify their techno-economic-environmental feasibility.

Second, several researchers have begun to investigate flexibility control in both normal and zero-energy buildings to reduce the electricity bill and integrate different renewable energy sources to compensate for the mismatch between renewable energy generation and demand. However, the current research in this direction focuses more on the use of thermal systems in buildings, such as heat pumps, cooling and heat storage tanks, and the optimal control of thermal systems. Their economic analyses frequently result in changes in the annual electricity bills. A few studies have incorporated other energy storage systems such as batteries and investigated the techno-economic performance of the systems over the entire life cycle.

Third, as different regions have proposed demand response or demand-side management projects for high loads of electricity consumption during peak periods, researchers have explored the impact of applying these projects through various control strategies on building bills and total peak loads. However, their current

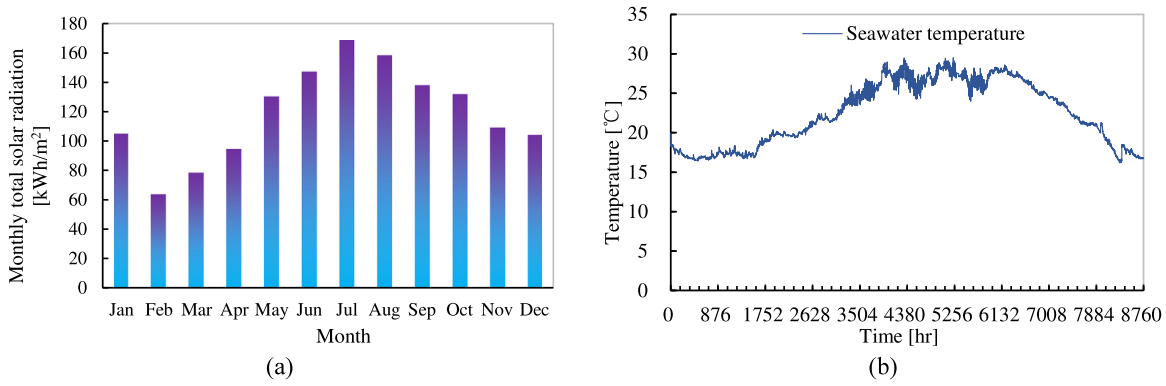

Fig. 1. Weather data: (a) monthly total solar radiation on the horizontal surface and (b) seawater temperature.

research focuses on the application of demand response projects using different intelligent control methods to reduce annual electricity bills, primarily in single residential buildings. The research on the use of energy storage systems and corresponding controls for larger buildings to apply the region's demand response program and investigate their techno-economic performance over the life cycle is limited.

Based on these three scientific gaps, this study investigated the impact of a flexibility enhancement approach for a zero-energy office building supported by ocean energy on the techno-economic performance. Moreover, it examined the impact of these flexibility controls on the economic performance of the target building over one year and its entire life cycle following the application of the region's demand response project. The novelty of this study is that, first, a coastal office building achieved the goal of a zero-emission building and was profitable throughout its life cycle through the incorporation of FPV panels, tidal stream generators (TSGs), and sea-source cooling systems. Second, the impact on the techno-economic performance of the system was investigated through different control measures to enhance flexibility using flexibility sources in the system. Third, the impact of different control methods on system performance was analysed through simulations after the application of the Peak Demand Management (PDM) programme in the Hong Kong region. In this study, the main variable was battery capacity. The techno-economic performance of the system under flexible control was investigated using two control methods. After the introduction of the PDM programme, its impact on the economic performance of the system and the possibility of achieving a neutral economic performance of the system at different percentages of renewable energy generation over a 20-year life cycle without a feed-in tariff were explored. Furthermore, two suggestions were proposed for the refinement of the current policy to improve economic performance without a feed-in tariff. The remainder of this paper is organised as follows. In Section 2, the weather, building demand, and simulation environment are presented. Descriptions of the building services, integrated ocean system, utility tariff model, and PDM programme are presented in Section 3. The detailed analysis criteria are presented in Section 4. In Section 5, the simulation results and discussions are presented. Finally, the conclusions are presented in Section 6.

2. Weather, coastal building demands, and simulation environment

The investigation of flexibility control and enhancement was based on a case study established in a previous study. The case study was a simulated hypothetical ocean-energy-supported zero-emission office building using a hybrid FPV system and TSGs. This section presents the weather data used in this study, the various demands of the original coastal office building, and the simulated environment.

The location of the case study was Ma wan, Hong Kong. The weather condition of Hong Kong is subtropical. The weather file of Hong Kong from the simulation software provided essential hourly weather input data for building energy simulations, including ambient temperature and humidity. Hourly solar radiation data were also included for the energy simulation of the FPV system (SEL, 2017; MeteotestAG, 2021). Based on data from the weather file, the annual total solar radiation on the horizontal surface was 1423 kWh/m^2. The monthly values of total solar radiation on the horizontal surface are shown in Fig. 1(a). The maximum monthly solar radiation was observed in the summer month of July (168.5 kWh/m^2), and the minimum in February (63.9 kWh/m^2), which corresponds with the climate of Hong Kong.

The seawater temperatures used in the sea-source cooling system and FPV system were provided by the Hong Kong Observatory. The seawater temperature data were monitored at the Waglan Island seawater area and recorded at one datum per hour. Fig. 1(b) shows the hourly seawater temperatures.

The tidal stream data used to simulate the energy generation of the TSG system were provided by the Hydrographic Office of the Marine Department (HKHO, 2017), and the interval between the data was 0.25 h. The data were generated by the Hong Kong Tidal Stream Prediction System based on the tidal components generated from the updated Hong Kong Tidal Atlas Model. According to the Hydrographic Office, the average difference in the current peak speed ranges from 0.03 to 0.21 m/s, while the average phase difference in peak velocity is approximately 17 min based on the comparison of the predicted data with actual field observed data (HKHO, 2017). The tidal data monitoring and recording site is located at Kap Shui Mun, near Ma wan, and its location on the map is shown in the Google screenshot in Fig. 2(a). The tidal data used for the simulation were tidal velocities, whose monthly average and maximum values are presented in Fig. 2(b). Owing to the characteristics of the tides, the average monthly tidal velocity is relatively constant, ranging from 0.76 to 0.84 m/s.

The target rectangular office had ten office floors and one underground parking floor, which was established in a previous study (Cao, 2019). Each floor had the same size of 480 m^2 and a floor height of 3 m. Building envelopes, insulation, and other service systems were designed based on the Performance-based Building Energy Code of Hong Kong (EMSD, 2007). According to the Hong Kong Green Office Guide (HKGBC, 2016), to reduce solar heat gain through glazing, we set the window-to-wall ratio of

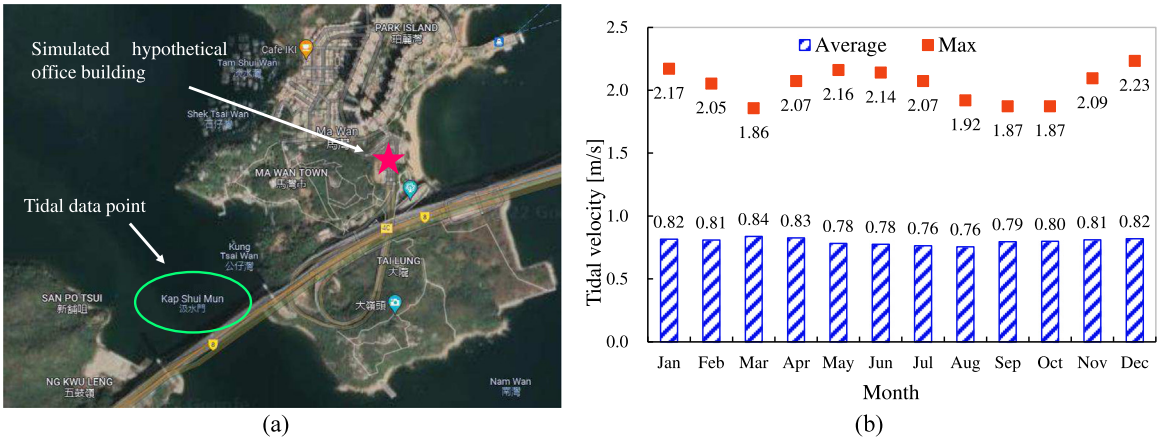

Fig. 2. Tidal data information: (a) tidal stream prediction point location and (b) monthly tidal velocity at the selected point.

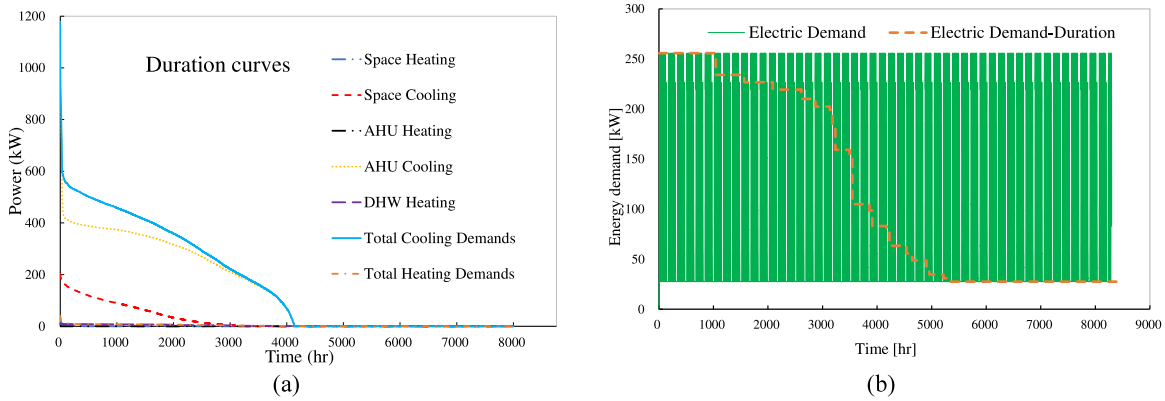

Fig. 3. Duration curves of the (a) cooling, (b) heating, and (c) electric demands of the target office building.

Table 1
Cooling, heating, and electric demands of the target office building.

	AHU cooling	Space cooling	Total cooling	AHU heating	Space heating	DHW heating	Total heating	Electrical demand
Total Energy (kWh/m^2)	223.4	38.22	261.6	0	0.39	4.47	4.86	191.3
Peak power (kW)	1177.8	204	1177.8	0.55	39.34	8.81	39.82	255.8

the external envelope to 0.21. The annual internal gain of the lighting system and equipment including devices and elevators were 58.6 and 104.3 kWh/m^2, respectively. The location of the office building considered in this study is shown in Fig. 2(a). The annual total energy demands and peak power demands of the air handling unit (AHU) cooling, space cooling, AHU heating, space heating, domestic hot water (DHW) heating, and electrical energy demands of the original coastal office building without any energy-saving strategies and renewable energy generation system were simulated (Table 1). The duration curves are shown in Fig. 3. The electrical energy demands of the office building shown in Table 1 and Fig. 3(b) include the electrical energy demands of all systems in the building, except for the cooling and heating systems.

The case study in the previous study was built in the TRNSYS 18 simulation environment (UW-Madison, 2021). As an open modular structure with open-source code, TRNSYS 18 is a dynamic energy simulation software that can simulate all types of energy systems and renewable generation using built-in models and an equation box with feasible equations. TRNSYS enables researchers to simulate the performance of an entire energy system by splitting the system into individual components or models. Therefore, this software is suitable for analysing single-building, local, and community energy systems (EnergyPlan, 2021). To maintain a stable simulation, we set the time step of the simulation in TRNSYS to 0.25 h.

3. Building services, integrated ocean energy system, and business models

3.1. Basic components, control principles, and associated flexibility sources

The main sections of this hybrid system include renewable energy systems, energy consumption equipment and service systems in buildings, and energy storage systems. A brief schematic of the system is shown in Fig. 4. The service systems include AHU cooling (AC), space cooling (SC), and DHW systems. The energy-consuming equipment includes water-cooled chillers in both AC and SC systems, auxiliary electric heaters in the DHW system, lighting systems, lifting systems, and office electric devices. The hybrid renewable energy system primarily consists of three parts.

The first part is the seawater cooling system, which is shown at the top of Fig. 4. The objective of this system is to decrease the energy consumption of the cooling system by utilising the ocean thermal energy (OTE). To achieve this, submerged heat

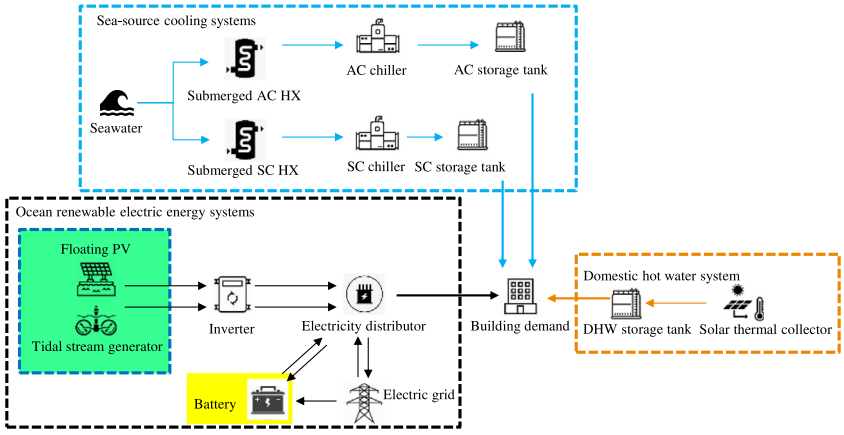

Fig. 4. Schematic of the coastal zero-energy office building with the hybrid ocean system.

exchangers (HX) are used instead of cooling towers in conventional refrigeration systems to connect the water-cooled chillers in both the AC and SC systems. Cooling storage tanks are also used in both cooling systems as energy storage units and were charged by water-cooled chillers. The second system is the DHW system, which is shown on the right side of Fig. 4. Based on the target building being an office building that only requires a DHW system, and because the sea source cooling system omits the cooling tower that is frequently placed on the roof, the roof area can be used to install solar thermal collectors to harness the solar energy supporting the DHW system. Therefore, the DHW storage tank is charged by both solar thermal collectors and auxiliary electric heaters. Third, the ocean renewable electric energy generation system, including FPV and TSG systems, is depicted on the left and highlighted in green. The FPV system uses PV panels with floating structures on the sea surface to harness solar energy, and the TSG system uses a hydrokinetic turbine in the seawater to utilise tidal energy. This system also incorporates stationary batteries as an additional energy-storage device and an effective source of flexibility, highlighted in yellow in the schematic diagram. Based on our preliminary investigation, although the cooling storage tanks of AC and SC systems can be used as flexibility sources, they have an insignificant impact on the operational cost. Therefore, stationary batteries served as the only flexibility source responding to the smart grid-based control in this study.

3.2. Ocean renewable electric energy system

3.2.1. Floating photovoltaic system

As a more common renewable energy option, systems using solar energy have been selected as a source to generate energy output for the target office building. Because the conversion efficiency of existing technologies for harnessing solar energy is not significant, large areas of land are required to install solar PV panel systems to satisfy the energy demand of a building. However, owing to the high urban density and large population volumes in Hong Kong, land resources are very limited, and the cost of land is very high. Hence, buildings in Hong Kong are frequently high-rise and closely spaced, and the shadows of the buildings prevent neighbouring buildings from receiving solar radiation. Therefore, the use of both traditional solar PV panel systems installed in open spaces near buildings and more innovative solar PV panels installed on the building envelope can be challenging in Hong Kong. As the subject of the study is a coastal office building and as a coastal city, Hong Kong has a 456 km coastline and sea area of 1644 km^2 (EPD, 2005; LandsD, 2020), FPV systems installed in the sea area near the target building were selected for this study based on previous research (Zhou et al., 2022). The hypothetical locations of the FPV system and target building are shown in Fig. 5.

The main aim of developing FPV systems is to reduce the amount of land available for installing solar PV panels. To ensure the stability of floating solar PV panel systems mounted on floating platforms, i.e. to receive solar radiation at a more stable angle, most experimental or commercial projects are currently installed on the surface of calmer bodies of water such as reservoirs or lakes (Kumar et al., 2021). In recent years, an increasing number of pilot projects have installed FPV systems on the open sea (Greentechmedia, 2019; Intelligentliving, 2021; Oceansofenergy, 2020; SolarEdition, 2020). Meanwhile, owing to the more stable temperature of seawater compared with the ambient air temperature and lower surface seawater temperature in the hot summer months compared with the ambient temperature or the temperature near the building envelope, and because the FPV system is installed on the surface of seawater, the FPV system has a higher solar energy conversion efficiency (Kumar et al., 2021). In the TRNSYS simulation, the self-contained model Type 567 to describe the building integrated photovoltaic (BIPV) was selected as the simulation model, which was based on the five-parameter circuit model. This model was selected because it shows the effect of seawater temperature on the energy generation of FPV panels in simulations by including a parameter called the back surface temperature, which can demonstrate the benefits of FPV systems. Moreover, with reference to recent FPV projects on the open sea, the slope of the FPV panels was set at 0°, which was parallel to the calm sea surface, to avoid the risk of waves and wind changing the orientation of the FPV system and not adequately absorbing solar radiation (Intelligentliving, 2021; Statkraft, 2019). A commercial product called FU 260P (FuturaSun) was selected for this study (FuturaSun, 2017). The detailed parameters of this product under standard test conditions of 1000 W/m^2 and 25 °C are listed in Table 2.

Based on the previous study (Zhou et al., 2022), we selected the optimum technically performing case from all the hybrid renewable energy cases with different mix ratios, which was called G1C3 and included 3967 pieces of FPV panels. Therefore, the number of FPV systems in the hybrid renewable energy system of the zero-energy building case in this study was 3967. The installation cost of FPV panels was assumed to be 26520 HKD/ kW, and the annual operation and maintenance (O&M) cost was assumed to be 1.92% of the initial investment cost (Paixão

Table 2
Detailed parameters of PV panel product under the standard test conditions.

Name	Module power	Module efficiency	Dimensions	Glass
FU 260P	260 W	15.92%	1.65×0.99×0.035 m	Tempered, Transparent, 3.2 mm

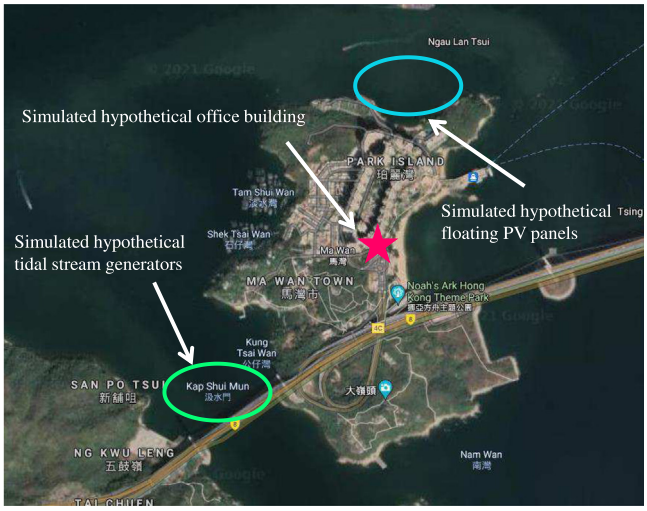

Fig. 5. Simulated hypothetical position of the entire system.

Martins, 2019; NREL, 2021). The average USD to HKD exchange rate from 2015 to 2019, which was 7.8, was used in this study to standardise the units (World Bank, 2021a).

3.2.2. Tidal stream generation system

Another renewable energy system in this hybrid system is the TSG system, which places hydrokinetic turbines in tidal streams to capture tidal energy from moving water masses (Fraenkel, 2006). As a form of hydrokinetic power, tidal energy is one of the more common types of ocean energy produced by the surge of ocean waters during rising and falling tides. Tides are changes in the level of the ocean caused by the gravitational attraction between the sun and moon acting on the ocean. Tidal energy is highly predictable in terms of its amount and timing, which can produce a steady and reliable stream of electricity. Considering the limited land resources and the high cost of land resources in Hong Kong, the TSG, which has a relatively simpler structure, was selected among the two common tidal energy technologies, tidal barrage and TSG. Based on the tidal stream data obtained and the geographical location of the office building, the location for the installation of the TSG was also assumed in this study, as shown in Fig. 5.

A hydrokinetic turbine is the core component of TSGs. Three typical tidal turbine structures are used to anchor the TSGs in specified locations: gravity base, mono-pile, and floating structures. In this study, based on the settings used in previous research, tidal turbines with floating structures were assumed to be used. This is because floating structures have several advantages, including flexibility, ease of maintenance, and relatively low cost, and the installation and removal of floating moored systems can be relatively rapid (Fraenkel, 2002). As an effective dynamic energy simulation software, TRNSYS 18 contains various built-in models for simulating different renewable energy systems. Although tidal power is one of the few renewable energy sources that do not have a built-in model in TRNSYS, this can be achieved using a suitable and feasible power-generation formula and equation box. In this study, a commercial product, the Neptune Proteus vertical-axis tidal stream power generator, was used to build the model. Based on the power curves and the generalised logistic function from Hardisty's research on this commercial product (Hardisty, 2012), the simulation function of a 250 kW Neptune Proteus TSG modelled in TRNSYS can be expressed as

$$P(t) = \frac{250}{\left(1 + 5.785e^{-0.122(v-1.3306)}\right)^{1/0.0325}} \quad ((1)\ \text{Hardisty, 2012})$$

where P(t) is the instantaneous power-generation output. As described in the previous subsection, a previously studied case, G1C3, was selected for this study. It contained two TSGs to form a zero-emission office building (Zhou et al., 2022). Therefore, two TSG systems were used in the hybrid renewable energy system for the zero-emission building case in this study. The installation cost of the TSG was assumed to be 19110 HKD/kW, and the annual O&M cost was assumed to be 5% of the capital cost (Chen, 2013) (NREL).

3.3. Electricity tariff model and peak demand management programme in Hong Kong

As an important part of the techno-economic analysis of a zero-energy building, the electricity tariff model used by the target office building in Hong Kong was the first step to be determined before calculating the economic criteria. The tariff model was selected from the 2021 electricity tariff table of CLP Power Hong Kong, Ltd. (CLP, 2021a). One of the electricity tariff models for buildings with high electricity consumption is the CLP bulk tariff. As an eight-storey office building with high electricity consumption, it satisfies the CLP bulk tariff requirement of at least 20,000 kWh per month, and the bulk tariff differentiates between peak and low-peak electricity costs. Therefore, the CLP bulk tariff was selected for this study. Table 3 lists the specific requirements and charge rates for the tariff model are listed in Table 3.

Based on the data in Table 3, a 2.5 times difference was observed in the demand charge between the on-peak and off-peak periods for this tariff model; therefore, there was considerable potential to reduce operating costs by conducting flexibility control between the on-peak and off-peak periods.

Meanwhile, as a CLP bulk tariff customer, the office building in this study was eligible to participate in CLP's PDM programme, an incentive mechanism for smart grid. This programme is similar to international demand response programmes in which rebates can be earned by reducing energy use during peak demand periods (CLP, 2021b). The aim of the programme is to encourage commercial customers to reduce their energy consumption during on-peak hours to reduce pressure on the grid. Customers can gain incentives when they join PDM events, which are held for up to 4 h between 11 am and 10 pm. Before the occurrence of these PDM events, CLP sends advance notice to the customer on the time and duration of the event if they are selected to participate in an upcoming event. The incentive rate for the PDM event is determined by the notification lead time, the data for which are presented in Table 4. In this study, the addition of the CLP PDM programme based on flexibility control was explored in terms of its impact on the economic performance of the systems.

CLP and the client agree on a mutually agreed "target" for hourly demand reduction, and while CLP welcomes customers to reduce their electricity demand by an amount greater than the target, they can only offer a maximum incentive payment for electricity demand reduction up to 150% of the target for

Table 3
Detail requirements and charge rates of CLP bulk tariff.

(a) Demand Charge				(b) Energy Charge		
On-Peak Period		Off-Peak Period		On-Peak Period		Off-Peak Period
Minimum on-peak billing demand: 100kVA				Total Monthly Consumption Block, Rate (Cents/Unit)		
Each of the first 650 kVA	Each kVA above 650	Each off-peak kVA up to the on-peak billing demand	Each off-peak kVA in excess of the on-peak billing demand	Each of the first 200,000 units	Each unit over 200,000	Each unit
68.4 HKD	65.4 HKD	0.0 HKD	26.8 HKD	75.3	73.7	67.6

Table 4
Incentive rates of the PDM programme based on the notification lead time.

Notification lead time	Event status	Incentive rates (HKD per kWh reduction)
≥24 h before the event	Executed	8
	Cancelled	8
≥4 h but <24 h before the event	Executed	13
	Cancelled	8

each event. CLP defines the total reduction in electricity demand achieved by the customer by calculating the difference between the baseline and actual electricity demand during the event period. This normalised baseline is the average electricity demand in the same period of the relevant event of the three highest electricity demand days in the ten preceding non-event days.

4. Analysis criteria

Several technical and economic analysis criteria were defined in advance to present the results and performance of the investigation of enhancing building energy flexibility in this study, and the definitions and generalised formulas of these applied criteria are presented in this section.

After exploring control strategies to enhance the energy flexibility of the building, the technical analysis was based on the evaluation of the flexibility controls to verify and demonstrate the effectiveness of the measures. Based on the previously described tariff model, we aimed to reduce peak demand and energy consumption by shifting power demand from the peak period to the off-peak period. Therefore, two criteria were proposed to demonstrate the performance of flexibility control strategies: the peak shaving indicator (PSI_{peak}) and off-peak valley filling indicator ($VFI_{offpeak}$). These two analysis criteria are determined by the duration curve of the peak and off-peak periods, and their brief diagrams are shown in Fig. 6.

In Fig. 6(a), area I represents the full peak-shaving potential to reduce the peaks in the peak period to the average power value, and area II represents the true amount of peak shaving obtained through the flexibility control measures. In Fig. 6(b), area I represents the potential to fill the entire valley below the average power value in the off-peak period, and area II represents the true amount of valley filling obtained through flexibility control measures.

The generalised equations of the two criteria can be expressed as

$$PSI_{peak} = \frac{\int_0^{t_{p,ref}} \left[P_{ref,p(t)} - P_{j,p(t)}\right] dt}{\int_0^{t_{p,ref}} \left[P_{ref,p(t)} - P_{avg,ref,peak}\right] dt} \quad (2)$$

$$VFI_{offpeak} = \frac{\int_{t_{op,ref}}^{t_{op,end}} \left[P_{j,op(t)} - P_{ref,op(t)}\right] dt}{\int_{t_{op,ref}}^{t_{op,end}} \left[P_{avg,ref,offpeak} - P_{ref,op(t)}\right] dt} \quad (3)$$

where '$t_{p,ref}$' is the temporal intersection of the demand duration curve and the average demand line of the reference case during the peak period, '$P_{ref,p(t)}$' is the demand duration curve of the reference case during the peak period, '$P_{j,p(t)}$' is the demand duration curve of the selected case (j) with flexibility control strategy during the peak period, '$P_{avg,\ ref,p(t)}$' is the average demand line of the reference case during the peak period, '$t_{op,ref}$' is the temporal intersection of the demand duration curve and the average demand line of the reference case during the off-peak period '$t_{op,end}$' is the instance when the demand duration curve of the reference case for the off-peak period has a value of 0, '$P_{ref,op(t)}$' is the demand duration curve of reference case during the off-peak period, '$P_{j,op(t)}$' is the demand duration curve of case (j) with a flexibility control strategy during the off-peak period, and '$P_{avg,\ ref,op(t)}$' is the average demand line of the reference case during the off-peak period. Greater PSI_{peak} and $VFI_{offpeak}$ values indicate better technical performance.

Furthermore, to investigate the impact of flexibility enhancement on the economic performance of the hybrid system, we used the net present value as the only economic criterion in the analysis, which can indicate the net cash flows after the payback period. In this study, economic performance was compared based on the reference case, which did not have any renewable energy generation input and was supplied only by the grid. Therefore, this economic criterion can be described as the relative net present value (NPV_{rel}). The equation for NPV_{rel} is

$$NPV_{rel} = \sum_{t=0}^{n=20} \frac{B_t - C_t}{(1+i)^t} \quad (4)$$

where 'B_t' is the relative benefit of period t that includes the profits and savings of the hybrid system relative to the reference case, 'C_t' is the relative cost of the hybrid system relative to the reference case during period t, 'n' is the useful lifetime of the project, and 'i' is the interest rate. The value of the interest rate was specified as 2.139% based on the five-year average value (2016–2020) of Hong Kong's real interest rate provided by the World Bank (World Bank, 2021b). A positive value represents money that can be earned over a 20-year period, whereas a negative value represents a loss over a 20-year period. The electricity price escalation ratio was considered when calculating NPV_{rel}. Based on the electricity tariff prices obtained from Hong Kong Energy Statistics for the last 20 years, the value of the electricity price escalation ratio was 0.01315 (C&SD, 2022).

5. Simulation results, analyses, and discussions

This section describes the flexibility control and the PDM programme investigations through TRNSYS simulations. The results obtained from these two investigations are presented, and their demonstrated techno-economic performance is discussed.

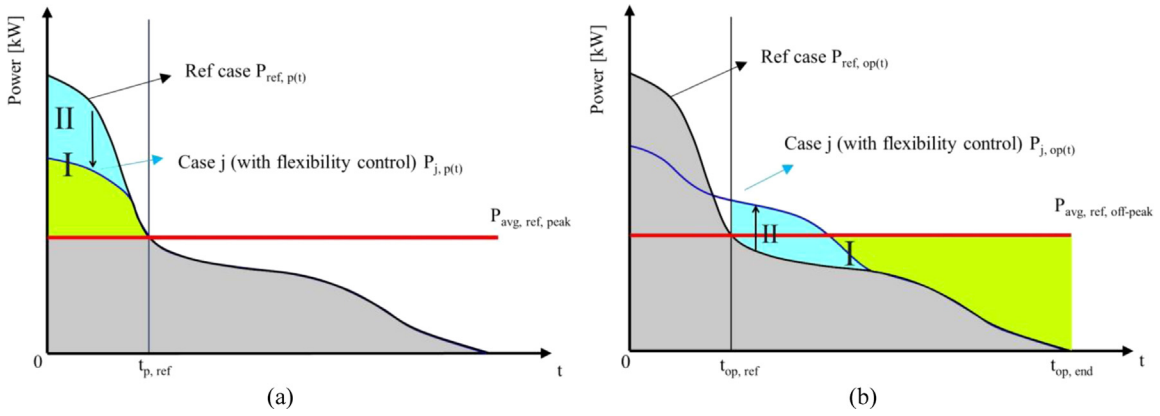

Fig. 6. Brief diagrams of (a) peak shaving indicator (PSI_{peak}) and (b) off-peak valley filling indicator ($VFI_{offpeak}$).

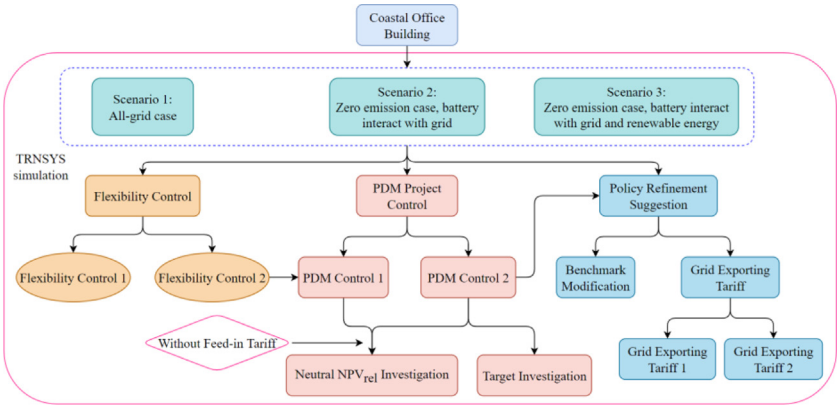

Fig. 7. Flow chart of the research steps and methodology.

Based on the results of these investigations, we discuss existing commercial tariff models and energy policies. Two approaches are proposed for the refinement of tariff models and PDM programme, and the feasibility of these two approaches was investigated through simulations. To estimate economic performance, we calculated the feed-in tariff for renewable energy set by the Hong Kong government based on the generation of renewable energy, which is 3 HKD per unit of generation (CLP, 2022). The investment cost of the battery was assumed to be 150 USD per kWh, which is 1170 HKD per kWh (Hsieh et al., 2019). To ensure proper operation, the batteries were assumed to be replaced every 10 years in this study. A flowchart of the research steps is shown in Fig. 7. The impact of flexibility control is presented in Section 5.1. Second, the impact of the PDM programme is investigated in Section 5.2, including the neutral NPV_{rel} investigation and target investigation. Furthermore, the investigation of policy refinement suggestions is demonstrated in Section 5.3, including benchmark modifications and grid exporting tariffs.

5.1. Investigation of flexibility control

Based on the previous description, the stationary battery is the only reliable source of flexibility in this hybrid system, and the flexibility control in this study was based on the interaction between the stationary battery and grid or renewable energy generation. The study of flexibility control was divided into three scenarios. In scenario 1 (S1), the target office building used only the sea-source cooling system and solar thermal collectors to reduce system energy consumption, no renewable energy generation system was incorporated, and all energy input was obtained from the grid; we called this scenario the all-grid case. In scenarios 2 (S2) and 3 (S3), based on S1, the previously mentioned ocean renewable energy generation system consisting of two TSGs and 3967 FPV panels was included in the system as the main energy input to the building, called the zero-emission case. In scenario 2 (S2), the stationary batteries were set to interact only with the grid, meaning that only the grid was used to charge the batteries. In scenario 3 (S3), the batteries interacted with both the renewable energy surplus and the grid, meaning that for a renewable energy surplus, the batteries would be charged first, and if the batteries were still available, the grid would be used to charge the batteries. The overall flexibility control strategies used in this study can be summarised as peak shaving and valley filling, whereby the stationary battery is charged during the off-peak period to reduce the energy demand peak during both the peak and off-peak periods. The value of the energy demand to be achieved to charge the battery during the off-peak period is called the charging line, and the target to reduce the energy demand by discharging the battery during the peak period is called the discharging line. As the energy demand varied from month to month, two control strategies were applied in the simulation: Flexibility Control 1 (FC1) and Flexibility Control 2 (FC2). In FC1, in a year, the charging line had the same value for each month, and the discharging line had the same value for each month. In FC2, in a year, the charging line differed for each month, and the discharging line differed for each month, but the charging and discharging lines were the same in the same month.

5.1.1. Scenario 1: All-grid case

The results for S1 are presented and discussed in this subsection. As previously described, the system in S1 did not include the

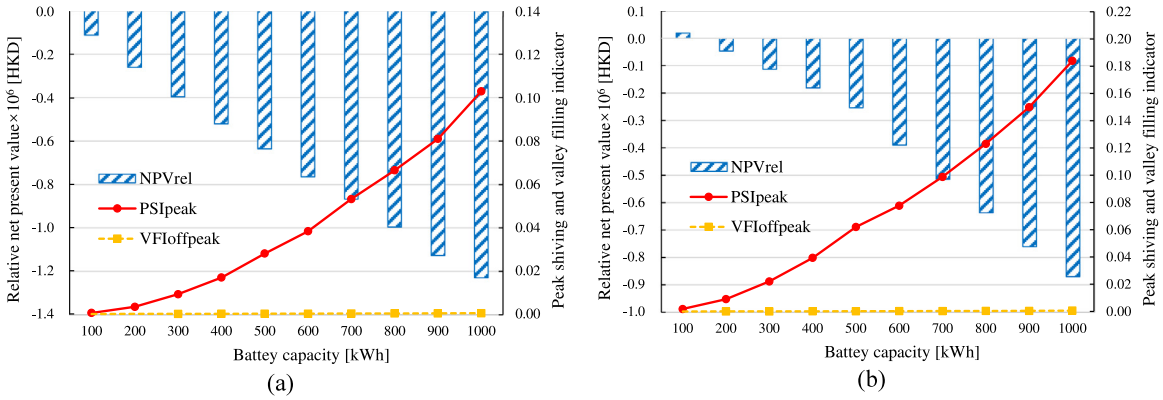

Fig. 8. Techno-economic performance of S1 under (a) FC1 (b) FC2 methods.

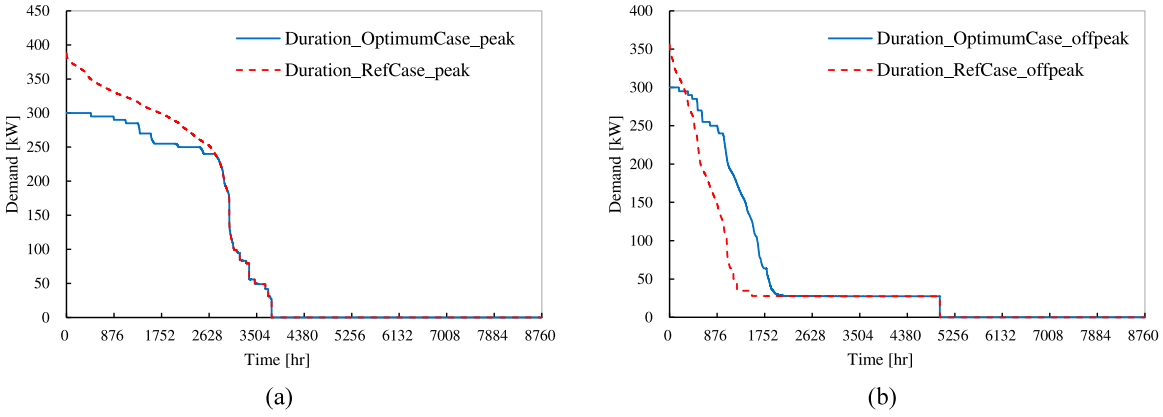

Fig. 9. Duration curves of optimum and reference case in S1 during the (a) peak period and (b) off-peak period.

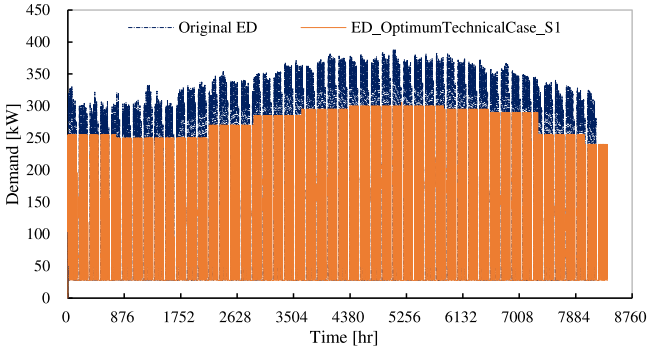

Fig. 10. Comparison between the annual original ED and the ED of the optimum technical performance in S1.

hybrid ocean energy system, and the energy demand of the office building was satisfied solely by the grid. In S1, the performance of the system was calculated and investigated for a total of 10 battery capacities, increasing from 100 to 1000 kWh, varying by 100 kWh each time. The indicators of techno-economic performance included the annual tariff, its reduction percentage based on the reference case, relative net present value (NPV_{rel}), peak shaving indicator (PSI_{peak}), and off-peak valley filling indicator ($VFI_{offpeak}$). The reference case was the all-grid case without any flexibility control. As observed from the results of the five indicators shown in Fig. 8, under the control of both methods, the annual tariff gradually decreased as the battery capacity increased, corresponding to a gradual increase in the annual tariff reduction percentage. The two technical performance indicators, PSI_{peak} and $VFI_{offpeak}$, also gradually increased. Although the annual tariff gradually decreased, the NPV_{rel} value also decreased owing to the high investment cost of the battery and replacement every 10 years. A comparison of the two control methods revealed that FC2 offered further improvements in both technical and economic performance compared with FC1. When the control method was FC1, NPV_{rel} was negative for all battery capacities, although the annual tariff could be reduced. When the control method was FC2, the annual tariffs were further reduced and the NPV_{rel} values increased, but the positive NPV_{rel} value only occurred with a 100 kWh battery, which was 0.18×10^5 HKD. Furthermore, the PSI_{peak} values in FC2 improved further, indicating that with FC2, the energy demand spikes in the peak period were more effectively reduced. The best technically performing case was the 1000 kWh battery in FC2 with PSI_{peak} and $VFI_{offpeak}$ values of 18.40×10^{-2} and 58.79×10^{-5}, respectively.

The duration curves of the case with optimum technical performance in S1 and the reference case in the peak and off-peak

periods are depicted in Fig. 9(a) and (b). The blue curves in the two plots are the duration curves of the case with the optimum technical performance in S1, and the red dashed line curves are the duration curves of the reference case. These duration curves show that the best technical performance in S1 effectively and significantly reduced the peak value of the energy demand during the peak and off-peak periods using a 1000 kWh battery. The part of the duration curve of the case with the optimum technical performance in Fig. 9(a) that does not overlap with the duration curve of the reference case has several sections of the same value, which shows that the energy demands during the peak period were perfectly controlled below the discharging line by FC2. A comparison between the energy demand (ED) of the optimum technical performance in S1 and the original ED without flexibility control is shown in Fig. 10, which clearly shows that FC2 was effective in reducing the peaks in the ED.

5.1.2. Scenario 2: Zero-emission case, battery interacts with the grid

In S2, the hybrid ocean energy system consisting of the TSG system and the FPV system introduced previously was incorporated based on the original S1. Batteries were also included as a source of flexibility, and they were only charged by the grid in this scenario. Ten different battery capacities were selected, beginning with 200 kWh and increasing in intervals of 200 kWh up to 2000 kWh. The reference case of S2 to calculate the reduction percentage was the all-grid case without any flexibility control, whereas the reference case to calculate NPV_{rel} was the zero-emission case without any battery or control. The data show that under FC1, the annual tariff continued to decrease as the battery capacity increased, and the reduction percentage of the annual tariff based on the reference case continued to increase, with a minimum annual tariff of 6.52×10^5 HKD per year when the battery was 2000 kWh. When FC2 was applied, the minimum annual tariff and the peak of its reduction percentage appeared for a battery of 1800 kWh, with 6.27×10^5 HKD and 18.02%, respectively. The annual tariff increased when the battery increased to 2000 kWh, because more electricity from the grid was spent during the off-peak period to charge the larger battery, and the savings from FC2 during the peak period could not cover this. This was also reflected in the greater increase in $VFI_{offpeak}$ and the higher slope of the $VFI_{offpeak}$ curve from 1800 to 2000 kWh (Fig. 11(b)). Similarly, when the battery capacity was the same, the technical and economic performance obtained with FC2 improved significantly compared with FC1. Although all NPV_{rel} values in S2 were positive, the NPV_{rel} values obtained from both FC1 and FC2 continued to decrease as the battery capacity increased, owing to the expensive battery investment costs. The best economic performance of the entire S2 was for a battery capacity of 200 kWh with FC2, with an NPV_{rel} of 23.94×10^6 HKD. The best technical performance was for a battery capacity of 2000 kWh with FC2, with the largest PSI_{peak} and $VFI_{offpeak}$ values of 37.76×10^{-2} and 14.02×10^{-2}, respectively.

The duration curves of the case with optimum technical performance in S2 and the reference case in the peak and off-peak periods are depicted in Fig. 12(a) and (b), respectively. The blue curves in the two plots are the duration curves for the case with the optimum technical performance in S2, and the red dashed line curves are the duration curves of the reference case. Similarly, the noticeable difference between the duration curves of the best technically performing and reference cases during the peak and off-peak periods at the beginning indicated that the peak value of the energy demand was effectively reduced during both the peak and off-peak periods. This proved the effectiveness of FC2. A comparison between the ED of the case with optimum technical performance in S2 and the original ED without flexibility control is shown in Fig. 13.

5.1.3. Scenario 3: Zero-emission case, battery interacts with the grid and renewable energy

The composition of the system in S3 was the same as that in S2, which incorporated the hybrid ocean renewable energy system and battery; the only difference was that in S3, the battery was charged by both the surplus renewable energy generated by the hybrid ocean renewable energy system and the grid. Ten different battery capacities were selected, starting with 200 kWh and increasing in intervals of 200 kWh up to 2000 kWh. The reference case of scenario 3 to calculate the reduction percentage was the all-grid case without any flexibility control, whereas the reference case to calculate NPV_{rel} was the zero-emission case without any battery or control. As Fig. 14 show, under the control of both methods, the technical performance indicators PSI_{peak} and $VFI_{offpeak}$ both increased as the battery capacity increased, whereas the economic performance indicators annual tariff and NPV_{rel} both decreased as battery capacity increased. Although the reduction in the annual tariff indicates improved economic performance, the high investment cost of the battery and the requirement to replace it every 10 years resulted in overall economic performance, as reflected by the NPV_{rel} value, which continued to deteriorate as the battery capacity increased. Meanwhile, comparisons demonstrated the improvement in both technical and economic performance obtained with FC2 compared with FC1. Therefore, both the best technically performing and optimum cases of economic performance used FC2. The case with the best technical performance used a 2000 kWh battery, the PSI_{peak} and $VFI_{offpeak}$ values were 41.18×10^{-2} and 9.40×10^{-2}, respectively. The case with the optimum economic performance used a 200 kWh battery, and the NPV_{rel} result was 23.99×10^6 HKD. Furthermore, the techno-economic performance of S3 was better than that of S2. This was because the direct output of surplus renewable energy to the grid could not benefit the system, whereas S3 used this surplus renewable energy to reduce operating costs and improve the performance of the system.

The duration curves of the case with optimum technical performance in S3 and the reference case in the peak and off-peak periods are shown in Fig. 15(a) and (b), respectively. The blue curves in the two plots are the duration curves of the case with the optimum technical performance in S3, and the red dashed line curves are the duration curves of the reference case. A comparison between the ED of the optimum technical performance in S3 and the original ED without flexibility control is shown in Fig. 16.

5.2. Investigation of the Peak Demand Management programme

As a customer using the bulk tariff model, the hybrid system in this study can be eligible to participate in CLP's PDM programme, an incentive mechanism for smart grid, as mentioned in the previous section. Based on the flexibility control achieved through batteries, as discussed in the previous subsection, the office building can reduce energy consumption and peak demand during peak periods by releasing the energy charged by the batteries during off-peak periods. By participating in this PDM programme, an incentive can be earned to improve the economic performance of the system by reducing energy consumption during peak event hours.

Therefore, the PDM programme was included in the energy simulation environment of the hybrid system to calculate the new annual electricity tariff and NPV_{rel} to demonstrate the impact of the PDM programme on the economic performance of the system. Because the battery was the only effective flexibility source in this system, the variable of the parametric study was the capacity

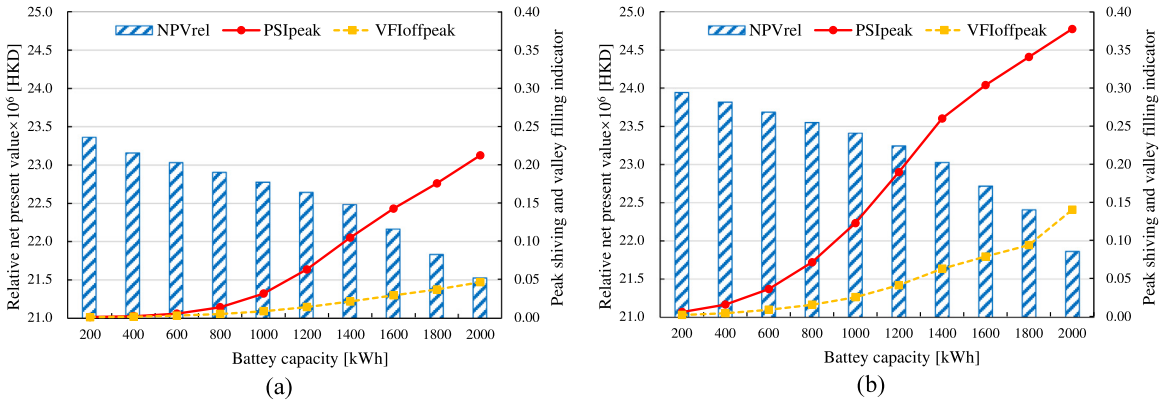

Fig. 11. Techno-economic performance of S2 under (a) FC1 and (b) FC2 methods.

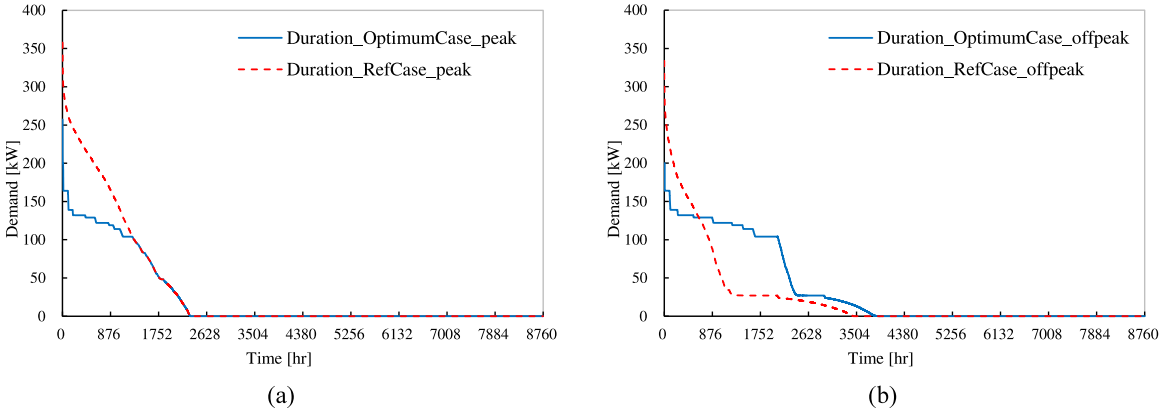

Fig. 12. Duration curves of optimum and reference case in S2 during the (a) peak period and (b) off-peak period.

Table 5
PDM cases and specific settings.

Name of PDM case	Event frequency	Notification lead time	Incentive rate [HKD/kWh]
C1	High frequency, 1 event per 2 days	≥4 h but <24 h before the event	13
C2	High frequency, 1 event per 2 days	≥24 h before the event	8
C3	Medium frequency, 1 event per 4 days	≥4 h but <24 h before the event	13
C4	Medium frequency, 1 event per 4 days	≥24 h before the event	8
C5	Low frequency. 1 event per 6 days	≥4 h but <24 h before the event	13
C6	Low frequency. 1 event per 6 days	≥24 h before the event	8

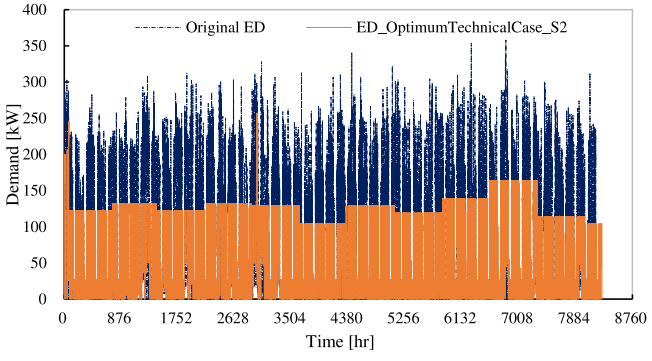

Fig. 13. Comparison between the annual original ED and the ED of the optimum technical performance in S2.

of the battery. Based on the previous flexibility control investigation, the investigation of the PDM programme was divided into three scenarios: scenario 1 (all-grid case), scenario 2 (zero-emission case) with the battery only interacting with the grid, and scenario 3 (zero-emission case), where the battery interacted with both the grid and renewable energy surplus. Two control methods were established to simulate the PDM programme. The first control method, called PDM Control 1, was based on the original flexibility of having different charging and discharging lines every month, without further control for the PDM programme. The second control method was called PDM Control 2, which was based on the original flexibility control, which increased the charging line to the maximum demand during the off-peak period each month, the battery did not discharge during the off-peak period to reduce peak demand and remained fully charged when

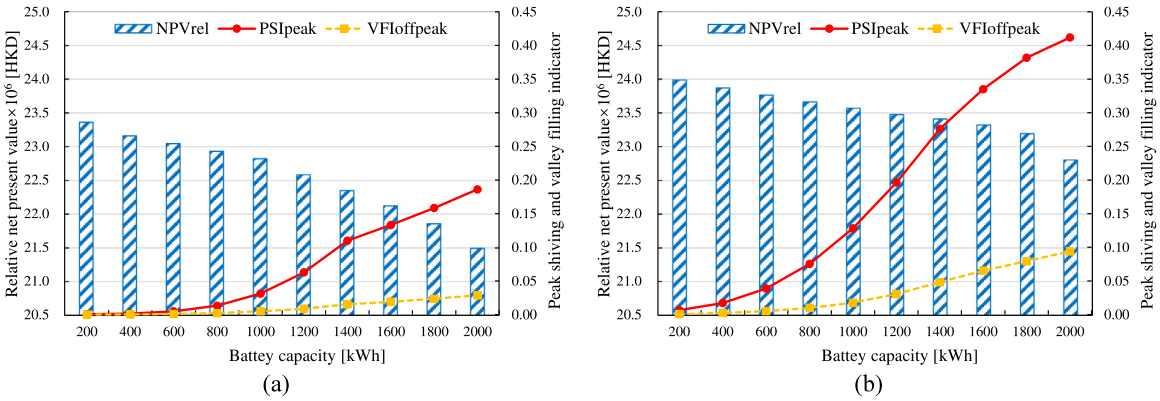

Fig. 14. Techno-economic performance of S3 under (a) FC1 and (b) FC2 methods.

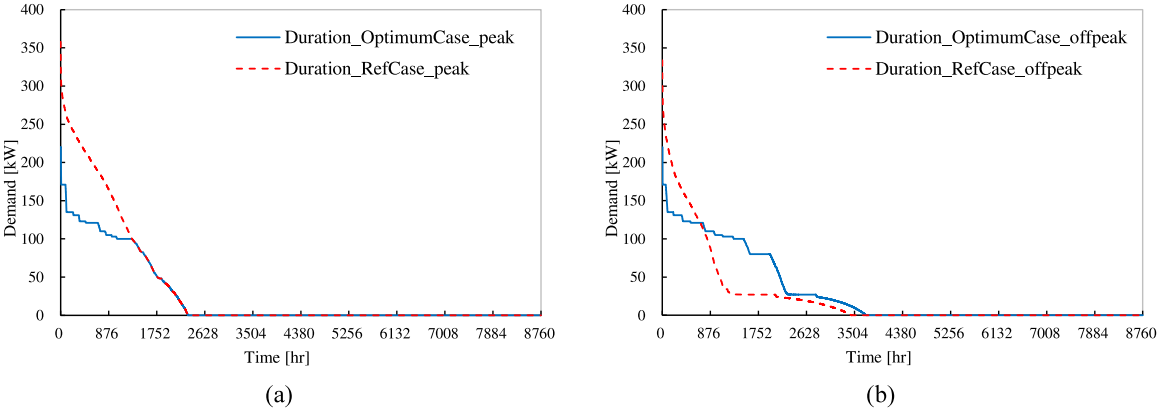

Fig. 15. Duration curves of optimum and reference case in S3 during the (a) peak period and (b) off-peak period.

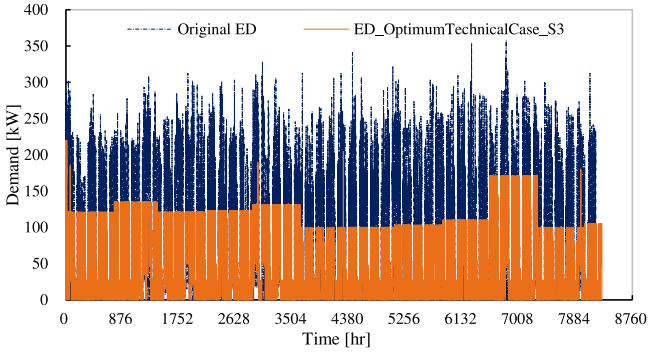

Fig. 16. Comparison between the annual original ED and the ED of the optimum technical performance in S3.

entering the peak period. When a PDM event occurs, the discharging line would be further reduced to increase the reduction in energy demand during the event period, resulting in more PDM incentives. This study created three different PDM event profiles determined by the frequency of event occurrences: high, medium, and low frequencies. The high-frequency event profile had an event every two days with a probability of 50%, the medium-frequency profile had an event every four days with a probability of 36%, and the low-frequency profile had an event every six days with a probability of 16.67%. The day on which the event occurred, start time, and maintenance time were determined using the stochastic function in Excel. Based on the frequency of these three PDM events and the two different notification lead times introduced previously, six different PDM cases can be formed for investigation: C1, C2, C3, C4, C5, and C6. The specific event frequency, notification lead time, and incentive rate for the six cases are shown in Table 5. The 'target' (kW) for the annual events was assumed to be unrestricted, which was equal to the maximum peak demand of the year. Based on the preliminary study, the difference between the NPV_{rel} calculated using different event profiles obtained using the stochastic algorithm for each year of the 20-year life cycle and NPV_{rel} calculated using the same event profile for each year was 1.91%, which was not significant. Therefore, the event profile would be the same for each year when calculating NPV_{rel}.

5.2.1. Scenario 1: All-grid case

For S1, similar to the previous flexibility investigation, the PDM programme explored a parametric study based on different battery capacities in TRNSYS. The battery capacities were first increased from 100 to 1000 kWh in intervals of 100 kWh. The impact of both PDM programme control methods on the economic performance of the system was demonstrated by the decrease in the operational cost and NPV_{rel}. The economic performances under PDM Controls 1 and 2 are presented in Tables 6 and 7, respectively. The variation trends of NPV_{rel} under PDM Controls

Table 6
Economic performance of PDM cases under PDM Control 1 in S1.

Battery capacity [kWh]		100	200	300	400	500	600	700	800	900	1000
C1	Annual tariff $\times 10^5$ [HKD]	14.97	14.96	14.99	15.04	15.08	15.11	15.13	15.14	15.14	15.13
	Reduction [%]	8.49	8.54	8.36	8.09	7.82	7.62	7.49	7.47	7.44	7.54
	$NPV_{rel} \times 10^6$ [HKD]	2.06	1.88	1.63	1.37	1.10	0.85	0.61	0.41	0.20	0.03
C2	Annual tariff $\times 10^5$ [HKD]	15.46	15.42	15.41	15.41	15.40	15.41	15.40	15.39	15.37	15.34
	Reduction [%]	5.52	5.74	5.81	5.83	5.84	5.82	5.85	5.95	6.04	6.24
	$NPV_{rel} \times 10^6$ [HKD]	1.27	1.14	0.96	0.77	0.58	0.37	0.18	0.01	−0.17	−0.32
C3	Annual tariff $\times 10^5$ [HKD]	15.72	15.69	15.67	15.64	15.63	15.62	15.59	15.56	15.53	15.50
	Reduction [%]	3.89	4.07	4.24	4.37	4.48	4.55	4.69	4.87	5.05	5.28
	$NPV_{rel} \times 10^6$ [HKD]	0.84	0.70	0.55	0.39	0.22	0.04	−0.13	−0.28	−0.43	−0.57
C4	Annual tariff $\times 10^5$ [HKD]	15.92	15.87	15.82	15.78	15.74	15.72	15.68	15.65	15.61	15.57
	Reduction [%]	2.69	2.99	3.28	3.54	3.79	3.92	4.12	4.35	4.57	4.84
	$NPV_{rel} \times 10^6$ [HKD]	0.53	0.41	0.29	0.17	0.04	−0.13	−0.28	−0.42	−0.56	−0.69
C5	Annual tariff $\times 10^5$ [HKD]	15.94	15.89	15.84	15.79	15.75	15.73	15.70	15.66	15.62	15.57
	Reduction [%]	2.55	2.87	3.17	3.46	3.72	3.87	4.06	4.28	4.52	4.80
	$NPV_{rel} \times 10^6$ [HKD]	0.49	0.38	0.27	0.15	0.02	−0.14	−0.29	−0.43	−0.57	−0.70
C6	Annual tariff $\times 10^5$ [HKD]	16.05	15.99	15.93	15.87	15.82	15.79	15.75	15.71	15.67	15.62
	Reduction [%]	1.86	2.25	2.62	2.98	3.32	3.51	3.73	3.99	4.24	4.55
	$NPV_{rel} \times 10^6$ [HKD]	0.31	0.22	0.12	0.02	−0.08	−0.24	−0.38	−0.51	−0.65	−0.76

1 and 2 are shown in Fig. 17(a) and (b), respectively. Based on the annual tariff results and reduction percentage in Table 6, in the cases of PDM Control 1, the annual tariff results in C1 increased and then decreased slightly as the battery capacity increased. In the other five cases, the annual operating costs gradually decreased as the battery capacity increased. However, the variation in the reduction percentage was insignificant at approximately 1% to 2%. Under PDM Control 1, the positive effect of the PDM programme on the economic performance of the system was greater when the battery capacity was lower. The reason for this was that the PDM model specifies the benchmark for calculating the PDM energy consumption reduction as the average value of the three maximum energy demands at the same period of the day in the ten preceding non-event days. In the original flexibility control, the monthly charging and discharging lines were reduced as the battery capacity increased, and the value of the energy demand was successfully reduced below the charging and discharging lines. This means that, as the battery capacity increased, the benchmark for calculating the energy demand reduction also reduced, reducing the incentive from the PDM programme. Meanwhile, owing to the high battery investment cost caused by replacing the battery every 10 years, the NPV_{rel} of cases C1 to C6 decreased with increasing battery capacity (Fig. 17(a)). From C3 to C6, the NPV_{rel} results even had negative values when the battery capacity was greater than 500 kWh.

When PDM Control 2 was applied to S1, the economic performance of the system was completely different from that of PDM Control 1. As shown in Table 7, the annual tariff for C1 to C6 decreased as the battery capacity increased. The largest reduction in annual tariff was observed in C1, where the annual tariff could be reduced by 3.95×10^5 HKD when the battery increased from 100 to 1000 kWh, and the reduction percentage could reach 32.90%. C6 had the smallest reduction in annual tariff when the battery increased from 100 to 1000 kWh, with a reduction of 1.24×10^5 HKD in annual tariff and a reduction percentage of 7.15%. Furthermore, owing to the increased incentives gained as a result of the control exercised on PDM programme, the economic performance of PDM Control 2, based on the reduction of annual tariff and NPV_{rel}, improved significantly compared with PDM Control 1. As shown in Fig. 17(b), the general trend of NPV_{rel} variation for C1 to C5 increased with battery capacity, except for C6, where the NPV_{rel} curve increased and then decreased as the battery capacity increased, with a peak of 0.28×10^6 HKD occurring at 400 kWh.

When the battery capacity increased to 900 and 1000 kWh, the NPV_{rel} of C6 became negative at -0.04×10^6 and -0.16×10^6 HKD, respectively. Based on this NPV_{rel} variation curve, the battery capacity was increased to 2000 kWh, with a single increase of 200 kWh, to investigate the economic performance. The annual tariff from C1 to C6 was further reduced as the battery capacity increases. The variation curve of NPV_{rel} for a single 200 kWh increase in battery capacity from 200 to 2000 kWh is shown in Fig. 17(c). By comparing Fig. 17(b) and (c), we observed that when the battery capacity increased to 2000 kWh, the NPV_{rel} of C1 to C5 changed in a comparable manner; both continued to increase, whereas the NPV_{rel} of C6 continued to decrease after a peak at 400 kWh.

5.2.2. Scenario 2: Zero-emission case, battery interacts with the grid

In S2, the target office building became a zero-emission system with the application of the hybrid ocean renewable energy generation system. Batteries would only be charged by the grid; the surplus renewable energy generation would be directly exported to the grid. Based on the previous flexibility investigation, the battery capacities were increased from 0 to 2000 kWh to investigate the impact of the PDM programme on the economic performance of the system in intervals of 50 kWh between 0 and 200 kWh, and intervals of 200 kWh between 200 and 2000 kWh. The economic performance under PDM Control 1 is presented in Table 8, whereas the economic performance under PDM Control 2 is presented in Table 9. The variation trends of NPV_{rel} under PDM Controls 1 and 2 are shown in Fig. 18(a) and (b), respectively.

When the battery capacity was 0, for both PDM Controls 1 and 2, the annual tariff decreased by 51.55%, 31.62%, 30.88%, 18.90%, 13.95%, and 8.48% from C1 to C6, respectively, compared with the reference case. As described in the previous section, renewable energy generation systems can be considered a source of reducing the energy import from the grid during the PDM event period. Therefore, when the hybrid marine energy system was incorporated into the office building, it could cover part of the energy demand during the PDM event period, resulting in a certain amount of PDM reduction and earning incentives compared with the all-grid case. When the control method was PDM Control 1, the results of the annual tariff and its reduction percentage in Table 8 show that, as the battery capacity increased, the annual tariff first decreased and then increased, and the reduction percentage first increased and then decreased for all six cases. For C1, the battery capacity capable of achieving a minimum annual tariff and maximum reduction percentage

Table 7
Economic performance of PDM cases under PDM Control 2 in S1.

Battery capacity [kWh]		100	200	300	400	500	600	700	800	900	1000	1200	1400	1600	1800	2000
C1	Annual tariff $\times 10^5$ [HKD]	14.93	14.74	14.40	13.81	13.33	12.83	12.36	11.88	11.42	10.98	9.99	9.00	7.98	6.96	5.96
	Reduction [%]	8.77	9.87	12.01	15.56	18.55	21.59	24.47	27.35	30.22	32.90	38.91	44.99	51.19	57.47	63.58
	$NPV_{rel} \times 10^6$ [HKD]	2.13	2.22	2.59	3.32	3.88	4.47	5.02	5.57	6.11	6.60	7.76	8.94	10.15	11.39	12.58
C2	Annual tariff $\times 10^5$ [HKD]	15.43	15.27	15.01	14.61	14.18	13.83	13.49	13.14	12.80	12.45	12.39	11.78	11.16	10.53	9.91
	Reduction [%]	5.68	6.50	7.95	10.23	11.90	13.76	15.52	17.25	18.98	20.57	24.24	27.97	31.78	35.64	39.41
	$NPV_{rel} \times 10^6$ [HKD]	1.31	1.33	1.52	1.92	2.13	2.41	2.66	2.90	3.14	3.34	3.89	4.44	5.03	5.62	6.20
C3	Annual tariff $\times 10^5$ [HKD]	15.71	15.57	15.35	14.98	14.64	14.34	14.05	13.78	13.51	13.28	12.72	12.18	11.63	11.07	10.54
	Reduction [%]	3.99	4.81	6.16	8.42	10.50	12.35	14.10	15.79	17.44	18.84	22.23	25.57	28.94	32.31	35.59
	$NPV_{rel} \times 10^6$ [HKD]	0.87	0.89	1.04	1.44	1.78	2.05	2.30	2.54	2.76	2.91	3.39	3.85	4.32	4.79	5.23
C4	Annual tariff $\times 10^5$ [HKD]	15.91	15.79	15.60	15.32	15.04	14.81	14.59	14.37	14.16	13.95	14.01	13.67	13.33	12.99	12.66
	Reduction [%]	2.74	3.42	4.35	5.85	7.12	8.26	9.33	10.37	11.39	12.21	14.34	16.41	18.50	20.59	22.61
	$NPV_{rel} \times 10^6$ [HKD]	0.54	0.52	0.57	0.76	0.89	0.97	1.04	1.11	1.17	1.16	1.31	1.43	1.56	1.69	1.80
C5	Annual tariff $\times 10^5$ [HKD]	15.93	15.82	15.68	15.47	15.29	15.12	14.99	14.86	14.74	14.64	14.35	14.06	13.77	13.48	13.20
	Reduction [%]	2.62	3.29	4.15	5.43	6.55	7.56	8.36	9.16	9.88	10.52	12.29	14.06	15.84	17.59	19.30
	$NPV_{rel} \times 10^6$ [HKD]	0.51	0.49	0.51	0.65	0.74	0.80	0.80	0.80	0.77	0.72	0.77	0.82	0.87	0.91	0.94
C6	Annual tariff $\times 10^5$ [HKD]	16.04	15.94	15.80	15.63	15.45	15.32	15.19	15.06	14.93	14.80	15.00	14.82	14.64	14.46	14.28
	Reduction [%]	1.90	2.48	3.12	4.01	4.76	5.43	5.92	6.40	6.80	7.15	8.28	9.41	10.54	11.64	12.73
	$NPV_{rel} \times 10^6$ [HKD]	0.32	0.27	0.24	0.28	0.27	0.24	0.15	0.07	−0.04	−0.16	−0.29	−0.41	−0.53	−0.66	−0.79

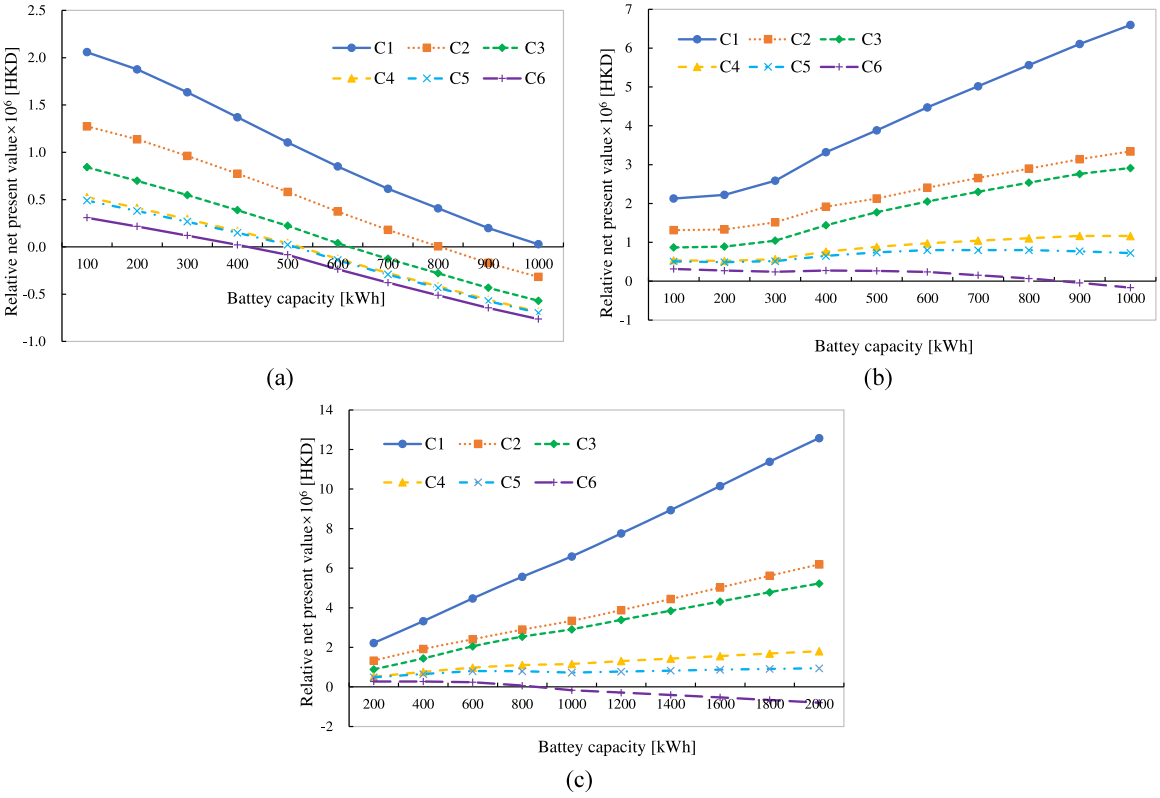

Fig. 17. NPV_{rel} curves of PDM cases in S1 with different battery capacities under (a) PDM Control 1 (b) PDM Control 2, and (c) PDM Control 2 (continued).

was 800 kWh, with an annual tariff and reduction percentage of 3.19×10^5 HKD and 58.33%, respectively, which were also the minimum annual tariff and maximum reduction percentage in all the six cases. In C2 and C3, the peak of the reduction percentage occurred at a battery capacity of 1000 kWh, whereas in C4, C5, and C6, the peak of the reduction percentage occurred at a battery capacity of 1800 kWh. This was because the benchmark used to calculate the PDM reduction was influenced by the discharging line during the peak period. As the battery capacity increased, the discharging line gradually decreased. Therefore, the benchmark also decreased, resulting in a decrease in the PDM incentive. The NPV_{rel} curves for PDM Control 1 are shown in Fig. 18(a). The curves were similar in all six cases owing to the high price of batteries and their replacement every 10 years, increasing and then decreasing as the battery capacity increased, with the peak occurring at a battery capacity of 50 kWh and a minimum value of 2000 kWh. The maximum NPV_{rel} value in the six cases occurred at 50 kWh for C1, which was 30.39×10^6 HKD.

When PDM Control 2 was applied, the results for the annual tariff and its reduction percentage in Table 9 showed that these two values varied in a similar manner to PDM Control 1, with the annual tariff decreasing and then increasing as the battery capacity increased, and the reduction percentage increased and then decreased. The difference with PDM Control 1 was that the turning point occurred at a larger battery capacity, frequently 1600 or 1800 kWh. Meanwhile, when larger batteries were selected, the annual tariff was lower under the PDM Control 2

Table 8
Economic performance of PDM cases under PDM Control 1 in S2.

Battery capacity [kWh]		0	50	100	150	200	400	600	800	1000	1200	1400	1600	1800	2000
C1	Annual tariff $\times 10^5$ [HKD]	3.70	3.46	3.42	3.39	3.36	3.26	3.20	3.19	3.24	3.35	3.51	3.60	3.67	3.86
	Reduction [%]	51.55	54.80	55.25	55.67	56.07	57.39	58.19	58.33	57.67	56.16	54.13	52.96	52.06	49.50
	$NPV_{rel} \times 10^6$ [HKD]	30.04	30.39	30.35	30.31	30.26	30.04	29.75	29.38	28.91	28.33	27.68	27.13	26.61	25.85
C2	Annual tariff $\times 10^5$ [HKD]	5.23	4.97	4.94	4.90	4.87	4.74	4.64	4.58	4.55	4.56	4.62	4.65	4.67	4.81
	Reduction [%]	31.62	34.98	35.47	35.93	36.37	38.00	39.29	40.17	40.54	40.31	39.63	39.22	38.97	37.07
	$NPV_{rel} \times 10^6$ [HKD]	27.58	27.95	27.91	27.87	27.83	27.64	27.42	27.14	26.79	26.37	25.89	25.43	24.99	24.32
C3	Annual tariff $\times 10^5$ [HKD]	5.29	5.03	4.99	4.96	4.92	4.80	4.71	4.65	4.62	4.64	4.68	4.70	4.72	4.87
	Reduction [%]	30.88	34.20	34.69	35.16	35.61	37.20	38.41	39.20	39.59	39.39	38.87	38.48	38.26	36.35
	$NPV_{rel} \times 10^6$ [HKD]	27.49	27.85	27.82	27.78	27.74	27.55	27.31	27.02	26.68	26.26	25.80	25.34	24.90	24.23
C4	Annual tariff $\times 10^5$ [HKD]	6.20	5.94	5.90	5.87	5.83	5.69	5.57	5.48	5.40	5.35	5.34	5.33	5.32	5.43
	Reduction [%]	18.90	22.30	22.81	23.30	23.78	25.58	27.12	28.40	29.42	29.99	30.24	30.30	30.48	28.97
	$NPV_{rel} \times 10^6$ [HKD]	26.01	26.38	26.35	26.31	26.28	26.11	25.91	25.68	25.42	25.10	24.73	24.33	23.94	23.32
C5	Annual tariff $\times 10^5$ [HKD]	6.58	6.32	6.28	6.24	6.20	6.06	5.94	5.83	5.74	5.68	5.64	5.61	5.59	5.69
	Reduction [%]	13.95	17.38	17.90	18.39	18.87	20.72	22.36	23.79	24.95	25.73	26.24	26.60	26.94	25.61
	$NPV_{rel} \times 10^6$ [HKD]	25.40	25.78	25.74	25.71	25.67	25.51	25.33	25.12	24.87	24.57	24.24	23.87	23.51	22.90
C6	Annual tariff $\times 10^5$ [HKD]	7.00	6.73	6.69	6.65	6.62	6.47	6.33	6.20	6.09	6.00	5.93	5.89	5.85	5.94
	Reduction [%]	8.48	11.95	12.48	12.98	13.49	15.43	17.24	18.92	20.41	21.58	22.46	22.99	23.51	22.37
	$NPV_{rel} \times 10^6$ [HKD]	24.72	25.11	25.08	25.04	25.01	24.86	24.69	24.51	24.31	24.06	23.77	23.43	23.08	22.50

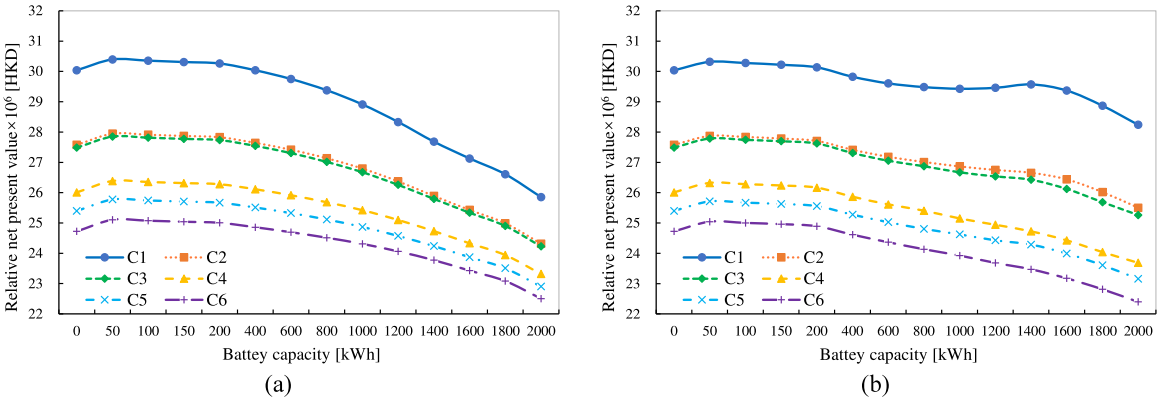

Fig. 18. NPV_{rel} curves of PDM cases in S2 with different battery capacities under (a) PDM Control 1 and (b) PDM Control 2.

method than under PDM Control 1, with a greater reduction percentage based on the reference case. For example, in C1, the turning point occurred at a battery capacity of 1600 kWh, with an annual tariff and its reduction percentage of 2.13×10^5 HKD and 72.12%, respectively. Compared with PDM Control 1 with a battery capacity of 1600 kWh, the reduction percentage increased by 19.15%, proving that the annual tariff had been further reduced. The reason for this was that the further reduction in demand during the event period through PDM Control 2 in some months reached its limit and could not be reduced any further, thus reducing the incentive from the PDM programme. Furthermore, in C1, when the battery capacity was less than 800 kWh, the NPV_{rel} results for PDM Control 2 were smaller than those for PDM Control 1, the difference being within 2×10^5 HKD. The battery capacity at which this occurred increased from C2 to C6, where the PDM incentive progressively reduced. This was because PDM Control 2 increased the charging line in the off-peak period, resulting in an increase in the off-peak tariff, and a small-capacity battery or a lower PDM incentive was not sufficient to cover this cost. For C1, C2, and C3, in which a sufficient incentive was combined with a larger battery capacity, the NPV_{rel} results for PDM Control 2 could be improved over PDM Control 1 (Fig. 18(b)). Although the NPV_{rel} curves of the six cases under PDM Control 2 were different from those of PDM Control 1, the overall trend was similar, with the peak NPV_{rel} occurring at a battery capacity of 50 kWh.

The previous NPV_{rel} results were calculated with a feed-in tariff to obtain a positive NPV_{rel} value. Because the feed-in tariff is a government subsidy to support the development of renewable energy, it can be considered a burden on the government economy. The focus of research on zero-energy buildings is the feasibility of zero-energy buildings with reduced or no feed-in tariffs. The economic performance of the system can be improved by earning incentives through the PDM programme and controlling the flexibility of the system itself. Therefore, this study used cases C1 to C6 from PDM Control 2 to investigate the percentage of renewable energy generation at which the system could achieve a neutral NPV_{rel} value after participating in the PDM programme. The NPV_{rel} results for a single 10% increase in the percentage of renewable energy generation from 0 to 100% in C1 to C6 without feed-in tariff are shown in Appendix A, the NPV_{rel} curves based on the percentage of renewable energy generated and the change in battery capacity are shown in Fig. 19. The specific numbers of TSGs and FPVs in the hybrid ocean energy system for each percentage are listed in Table 10. The results indicated that in the absence of the feed-in tariff, the neutral NPV_{rel} value occurred at low percentages of renewable energy generation owing to the expensive investment costs of renewable energy systems and the battery and O&M costs of ocean renewable energy systems. The frequency of PDM events, PDM incentive, and battery capacity are important factors influencing the NPV_{rel} results. In C1 with a high PDM event frequency, the neutral NPV_{rel} values occurred between 20% and 30% of the renewable energy generation when the battery capacity reached 2000 kWh. In C2, which also had high PDM event frequency but a reduced PDM incentive, the neutral NPV_{rel} value occurred

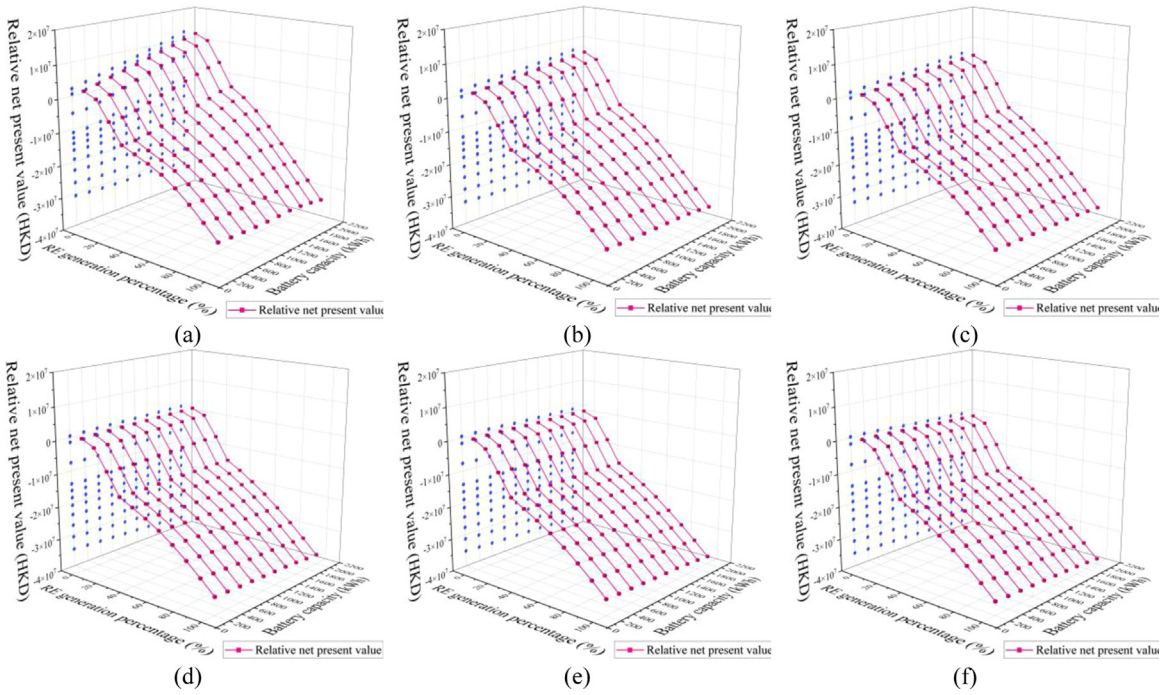

Fig. 19. NPV_{rel} curves with different battery capacities and RE generation percentages in (a) C1, (b) C2, (c) C3, (d) C4, (e) C5, and (f) C6 of S2.

Table 9
Economic performance of PDM cases under PDM Control 2 in S2.

Battery capacity [kWh]		0	50	100	150	200	400	600	800	1000	1200	1400	1600	1800	2000
C1	Annual tariff $\times 10^5$ [HKD]	3.70	3.50	3.46	3.44	3.43	3.37	3.26	3.08	2.86	2.59	2.26	2.13	2.19	2.33
	Reduction [%]	51.55	54.26	54.73	55.06	55.20	55.95	57.44	59.70	62.55	66.17	70.51	72.12	71.36	69.58
	$NPV_{rel} \times 10^6$ [HKD]	30.04	30.32	30.28	30.22	30.14	29.83	29.61	29.48	29.43	29.46	29.57	29.37	28.87	28.24
C2	Annual tariff $\times 10^5$ [HKD]	5.23	5.01	4.97	4.95	4.93	4.86	4.76	4.61	4.45	4.27	4.06	3.95	3.96	4.02
	Reduction [%]	31.62	34.44	34.95	35.32	35.50	36.40	37.79	39.66	41.77	44.19	46.86	48.34	48.24	47.40
	$NPV_{rel} \times 10^6$ [HKD]	27.58	27.87	27.84	27.79	27.71	27.41	27.18	27.01	26.87	26.75	26.65	26.44	26.02	25.50
C3	Annual tariff $\times 10^5$ [HKD]	5.29	5.07	5.03	5.00	4.98	4.93	4.84	4.70	4.57	4.40	4.21	4.14	4.16	4.18
	Reduction [%]	30.88	33.74	34.18	34.59	34.82	35.54	36.73	38.53	40.25	42.50	44.99	45.81	45.59	45.40
	$NPV_{rel} \times 10^6$ [HKD]	27.49	27.79	27.74	27.70	27.62	27.31	27.05	26.87	26.67	26.54	26.43	26.12	25.69	25.26
C4	Annual tariff $\times 10^5$ [HKD]	6.20	5.98	5.94	5.91	5.89	5.82	5.73	5.61	5.51	5.39	5.26	5.19	5.18	5.15
	Reduction [%]	18.90	21.85	22.30	22.74	22.99	23.85	25.05	26.64	27.91	29.56	31.19	32.08	32.26	32.64
	$NPV_{rel} \times 10^6$ [HKD]	26.01	26.32	26.28	26.24	26.16	25.87	25.61	25.41	25.15	24.94	24.72	24.43	24.04	23.69
C5	Annual tariff $\times 10^5$ [HKD]	6.58	6.35	6.32	6.28	6.27	6.19	6.09	5.98	5.85	5.71	5.55	5.47	5.46	5.48
	Reduction [%]	13.95	16.92	17.38	17.82	18.07	19.06	20.31	21.77	23.56	25.30	27.48	28.43	28.63	28.34
	$NPV_{rel} \times 10^6$ [HKD]	25.40	25.71	25.67	25.63	25.56	25.27	25.03	24.81	24.62	24.43	24.29	23.99	23.61	23.16
C6	Annual tariff $\times 10^5$ [HKD]	7.00	6.77	6.73	6.70	6.68	6.60	6.50	6.40	6.28	6.17	6.05	5.98	5.95	5.95
	Reduction [%]	8.48	11.50	11.96	12.42	12.68	13.70	14.95	16.33	17.90	19.26	20.88	21.78	22.18	22.18
	$NPV_{rel} \times 10^6$ [HKD]	24.72	25.04	25.00	24.96	24.89	24.61	24.37	24.13	23.93	23.68	23.47	23.17	22.81	22.40

Table 10
Specific numbers of TSG and FPV at different RE generation percentages.

G_{RE} percent [%]	Number of TSGs	Number of FPVs
100	2	3967
90	2	3462
80	2	2956
70	2	2451
60	2	1945
50	2	1440
40	2	934
30	2	428
20	1	467
10	0	506
0	0	0

between 10% and 20% of the renewable energy generated when the battery capacity reached 2000 kWh. In C6, with low PDM event frequency and a lower PDM incentive, the NPV_{rel} result was positive only when the battery capacity was less than 800 kWh and renewable energy generation was 0%. Continuing to increase the battery capacity would cause the system to have a negative NPV_{rel} even without the hybrid ocean energy system. These results indicated that under the existing utility business model and the PDM programme model, without the feed-in tariff, the Hong Kong office building with the hybrid ocean energy system would have difficulty in achieving a positive return over a 20-year lifecycle, and the economic feasibility would be unsatisfactory.

5.2.3. Scenario 3: Zero-emission case, battery interacts with the grid and renewable energy

In S3, the office building still incorporated a hybrid marine energy system. Compared with S2, the batteries in S3 were charged by both the grid and surplus renewable energy generation. Similarly, the battery capacities were increased from 0 to 2000 kWh,

Table 11
Economic performance of PDM cases under PDM Control 1 in S3.

Battery capacity [kWh]		0	50	100	150	200	400	600	800	1000	1200	1400	1600	1800	2000
C1	Annual tariff $\times 10^5$ [HKD]	3.70	3.44	3.40	3.37	3.34	3.23	3.16	3.14	3.17	3.25	3.36	3.39	3.36	3.53
	Reduction [%]	51.55	55.03	55.50	55.93	56.34	57.71	58.62	58.95	58.58	57.51	56.05	55.69	56.02	53.87
	$NPV_{rel} \times 10^6$ [HKD]	30.04	30.43	30.39	30.34	30.30	30.08	29.81	29.47	29.04	28.52	27.96	27.54	27.19	26.49
C2	Annual tariff $\times 10^5$ [HKD]	5.23	4.95	4.92	4.88	4.84	4.71	4.61	4.52	4.47	4.45	4.45	4.39	4.32	4.37
	Reduction [%]	31.62	35.22	35.72	36.20	36.66	38.35	39.77	40.86	41.54	41.78	41.86	42.55	43.56	42.86
	$NPV_{rel} \times 10^6$ [HKD]	27.58	27.98	27.95	27.91	27.87	27.69	27.48	27.24	26.94	26.58	26.21	25.92	25.65	25.03
C3	Annual tariff $\times 10^5$ [HKD]	5.29	5.01	4.98	4.94	4.90	4.78	4.67	4.60	4.54	4.52	4.50	4.45	4.38	4.51
	Reduction [%]	30.88	34.44	34.95	35.43	35.90	37.56	38.90	39.91	40.62	40.91	41.18	41.84	42.71	41.04
	$NPV_{rel} \times 10^6$ [HKD]	27.49	27.89	27.85	27.81	27.78	27.60	27.38	27.12	26.82	26.48	26.13	25.83	25.55	24.91
C4	Annual tariff $\times 10^5$ [HKD]	6.20	5.92	5.88	5.84	5.81	5.66	5.53	5.42	5.32	5.23	5.15	5.05	4.94	4.97
	Reduction [%]	18.90	22.55	23.07	23.58	24.08	25.95	27.64	29.15	30.49	31.57	32.71	34.03	35.38	34.96
	$NPV_{rel} \times 10^6$ [HKD]	26.01	26.42	26.39	26.35	26.32	26.16	25.99	25.79	25.57	25.32	25.08	24.86	24.64	24.05
C5	Annual tariff $\times 10^5$ [HKD]	6.58	6.30	6.26	6.22	6.18	6.03	5.90	5.77	5.66	5.56	5.45	5.32	5.21	5.30
	Reduction [%]	13.95	17.63	18.17	18.67	19.18	21.10	22.90	24.56	26.04	27.34	28.77	30.40	31.90	30.75
	$NPV_{rel} \times 10^6$ [HKD]	25.40	25.81	25.78	25.75	25.71	25.57	25.40	25.22	25.02	24.80	24.60	24.42	24.21	23.64
C6	Annual tariff $\times 10^5$ [HKD]	7.00	6.71	6.67	6.63	6.59	6.44	6.29	6.14	6.00	5.87	5.73	5.58	5.45	5.46
	Reduction [%]	8.48	12.20	12.75	13.27	13.79	15.82	17.79	19.70	21.52	23.22	25.07	26.99	28.72	28.63
	$NPV_{rel} \times 10^6$ [HKD]	24.72	25.14	25.11	25.08	25.05	24.91	24.77	24.62	24.47	24.29	24.14	24.00	23.82	23.27

Table 12
Economic performance of PDM cases under PDM Control 2 in S3.

Battery capacity [kWh]		0	50	100	150	200	400	600	800	1000	1200	1400	1600	1800	2000
C1	Annual tariff $\times 10^5$ [HKD]	3.70	3.48	3.45	3.43	3.41	3.35	3.23	3.04	2.80	2.51	2.17	2.16	2.21	2.28
	Reduction [%]	51.55	54.51	54.90	55.19	55.41	56.19	57.81	60.25	63.36	67.16	71.58	71.75	71.12	70.17
	$NPV_{rel} \times 10^6$ [HKD]	30.04	30.35	30.30	30.24	30.17	29.86	29.66	29.56	29.54	29.60	29.73	29.36	28.88	28.35
C2	Annual tariff $\times 10^5$ [HKD]	5.23	4.99	4.96	4.94	4.91	4.84	4.73	4.57	4.39	4.19	3.97	3.91	3.91	3.93
	Reduction [%]	31.62	34.69	35.12	35.46	35.73	36.67	38.19	40.24	42.60	45.22	48.07	48.84	48.91	48.59
	$NPV_{rel} \times 10^6$ [HKD]	27.58	27.91	27.86	27.81	27.74	27.45	27.24	27.09	26.98	26.90	26.83	26.53	26.14	25.69
C3	Annual tariff $\times 10^5$ [HKD]	5.29	5.05	5.02	4.99	4.97	4.91	4.81	4.66	4.52	4.34	4.12	4.12	4.14	4.16
	Reduction [%]	30.88	33.97	34.35	34.71	35.01	35.80	37.12	39.09	40.92	43.28	46.08	46.11	45.84	45.66
	$NPV_{rel} \times 10^6$ [HKD]	27.49	27.82	27.77	27.71	27.65	27.35	27.11	26.95	26.77	26.65	26.58	26.19	25.75	25.32
C4	Annual tariff $\times 10^5$ [HKD]	6.20	5.96	5.93	5.90	5.87	5.80	5.70	5.57	5.46	5.33	5.17	5.13	5.12	5.09
	Reduction [%]	18.90	22.07	22.48	22.85	23.18	24.12	25.46	27.22	28.60	30.35	32.35	32.88	33.11	33.39
	$NPV_{rel} \times 10^6$ [HKD]	26.01	26.35	26.30	26.25	26.19	25.90	25.67	25.49	25.25	25.05	24.89	24.55	24.18	23.81
C5	Annual tariff $\times 10^5$ [HKD]	6.58	6.33	6.30	6.28	6.25	6.17	6.06	5.94	5.79	5.64	5.45	5.40	5.38	5.40
	Reduction [%]	13.95	17.23	17.56	17.94	18.28	19.33	20.71	22.35	24.34	26.24	28.74	29.38	29.64	29.45
	$NPV_{rel} \times 10^6$ [HKD]	25.40	25.76	25.70	25.64	25.59	25.31	25.08	24.89	24.73	24.56	24.46	24.14	23.77	23.33
C6	Annual tariff $\times 10^5$ [HKD]	7.00	6.74	6.72	6.69	6.66	6.58	6.47	6.35	6.22	6.10	5.95	5.89	5.85	5.84
	Reduction [%]	8.48	11.80	12.15	12.54	12.89	13.98	15.35	16.91	18.69	20.21	22.15	23.00	23.55	23.59
	$NPV_{rel} \times 10^6$ [HKD]	24.72	25.09	25.03	24.98	24.92	24.65	24.42	24.22	24.04	23.82	23.65	23.35	23.01	22.60

in intervals of 50 kWh between 0 and 200 kWh, and intervals of 200 kWh between 200 and 2000 kWh. The economic performance under PDM Controls 1 and 2 are presented in Table 11 and Table 12, respectively, while the variation trend of NPV_{rel} curves under PDM Controls 1 and 2 are shown in Fig. 20(a) and (b), respectively.

With the application of PDM Control 1, the annual tariff and its reduction percentage varied similarly to that of S2. In all the six cases, the annual tariff decreased and then increased as the battery capacity increased, and the production percentage increased and then decreased. In C1, the turning point to achieve minimum annual tariff and maximum reduction percentage was at 800 kWh, with an annual tariff and reduction percentage of 3.14×10^5 HKD and 58.95%, respectively. In the other five cases (C2 to C6), the turning points appeared at 1800 kWh. The reasons for this variation were the same as those in S2. Based on the results and curves of NPV_{rel} shown in Table 11 and Fig. 20(a), the trend of NPV_{rel} for S3 was similar to that of S2, where NPV_{rel} increased and then decreased as the battery capacity increased, and the peak value occurred at 50 kWh. The maximum NPV_{rel} of S3 was 30.43×10^6 HKD, using a battery with a capacity of 50 kWh in C1. Comparing the two scenarios with PDM Control 1, we observed that the economic performance of S3 improved because the export of the renewable energy surplus directly to the grid cannot benefit the system, while the additional interaction of the battery with the renewable energy surplus reduces the cost of the electricity imported from the grid, thereby improving the economic performance.

For PDM Control 2, as shown in Table 12, the annual tariff and its reduction percentage varied in a similar manner to PDM Control 1, and as the battery capacity increased, the annual tariff first decreased and then increased. In C1, C2, and C5, the turning points appeared at 1800 kWh. In C3, the turning point was at 1600 kWh, whereas in C4 and C6, the turning points occurred at 2000 kWh. In C1, the minimum annual tariff was 2.16×10^5 HKD and its reduction percentage was 71.75%, which was also the minimum annual tariff and maximum reduction percentage among all the six cases. Similar to S2, in C1, C2, and C3, PDM Control 2 improved the economic performance of the system by reducing the operational cost and increasing NPV_{rel} when a larger battery capacity was selected compared with PDM Control 1. This can also be observed by comparing Fig. 20(a)

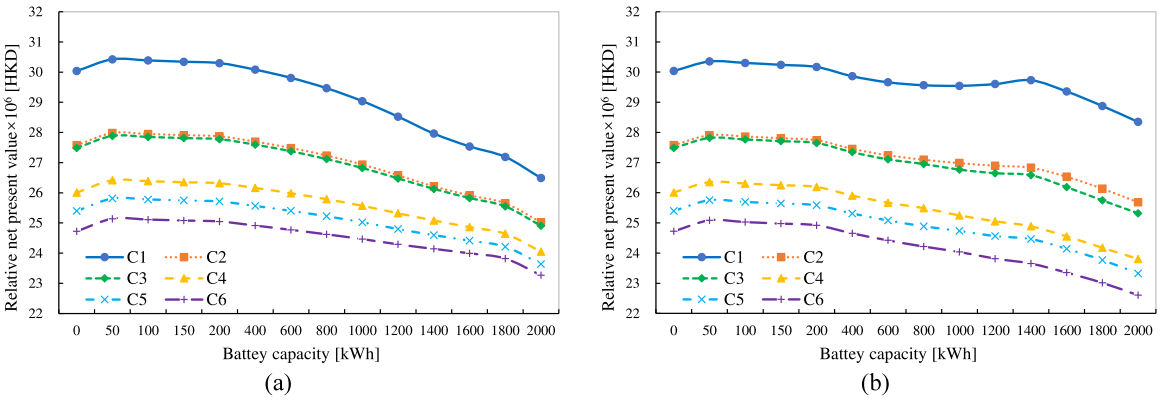

Fig. 20. NPV_{rel} curves of PDM cases in S3 with different battery capacities under (a) PDM Control 1 and (b) PDM Control 2.

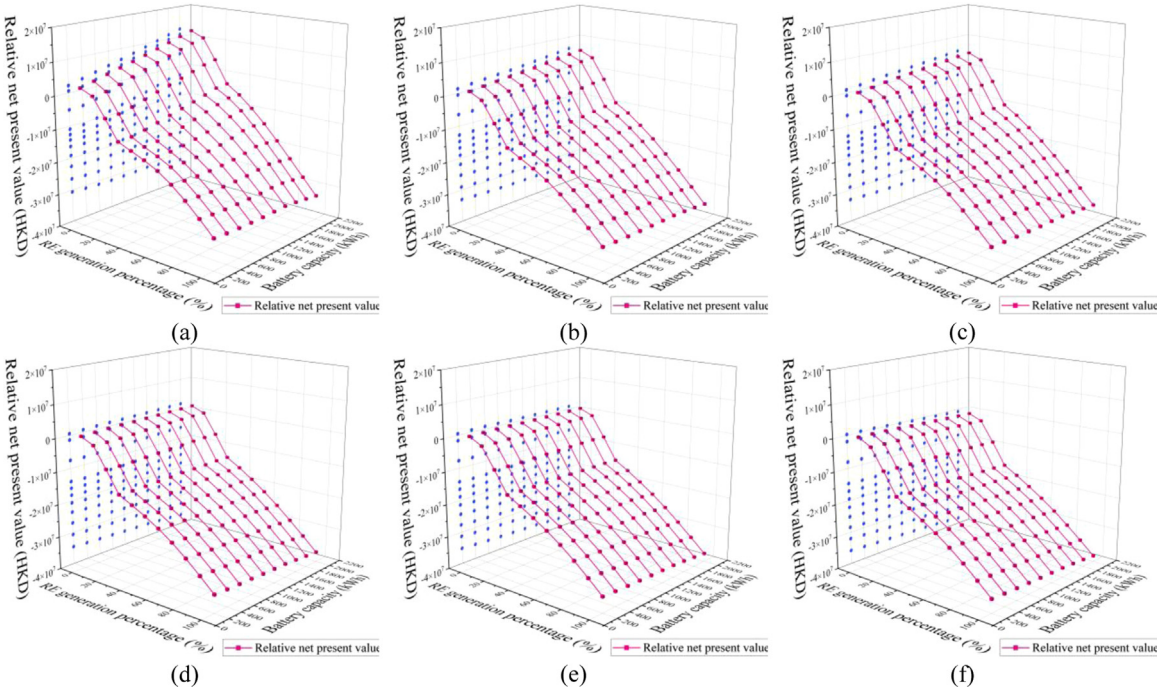

Fig. 21. NPV_{rel} curves with different battery capacities and RE generation percentages in (a) C1, (b) C2, (c) C3, (d) C4, (e) C5, and (f) C6 of S3.

and (b), where the latter parts of the curves for C1, C2, and C3 in Fig. 20(b) are significantly higher than those in Fig. 20(a) at larger battery capacities. The overall trend of the NPV_{rel} curve was similar for both control methods, with the NPV_{rel} curves increasing and then decreasing as the batteries became larger. The curves for C1, C2, and C3 descended and ascended again between 200 and 1400 kWh. As the battery exceeded 1400 kWh, the curve dropped again in all three cases. Meanwhile, the peak values of NPV_{rel} for all six cases occurred at 50 kWh, with a maximum NPV_{rel} of 30.35×10^6 HKD.

Similarly, all six cases of S3 were investigated in terms of the percentage of renewable energy generation at which a neutral NPV_{rel} value could be achieved without a feed-in tariff. The NPV_{rel} results for a single 10% increase in the percentage of renewable energy generation from 0% to 100% in C1 to C6 of S3 without the feed-in tariff are shown in Appendix B. The NPV_{rel} curves based on the percentage of renewable energy generated and the change in battery capacity are shown in Fig. 21. Compared with S2, similar findings and conclusions can be obtained, although the specific NPV_{rel} values were different. The maximum percentage of neutral NPV_{rel} values that could be obtained ranged from 20% to 30%; these results occurred in C1 with a battery capacity larger than 1400 kWh. In C2 and C3, when the battery was less than 600 kWh, the percentage of neutralised NPV_{rel} values that could be obtained was between 0% and 10%, and by continuing to increase the battery, this result could increase to between 10% and 20%. In C4 and C5, neutralised NPV_{rel} values occurred between 0% and 10% for most battery capacities. In C6, with the least PDM incentive, when the battery capacity was greater than 1000 kWh, a positive NPV_{rel} could not be achieved even without the hybrid ocean energy system owing to the expensive battery investment costs. A similar conclusion can be drawn that under the existing utility business model and PDM programme model, without the feed-in tariff, the Hong Kong office building with the hybrid ocean energy system would have difficulty achieving a positive return over a 20-year lifecycle.

Table 13
NPV_{rel} results of PDM cases with different targets.

PDM case	Target [kW]	50	100	150	200	250
C1	$NPV_{rel} \times 10^7$ [HKD]	2.65	2.83	2.83	2.83	2.83
	Difference %	6.61	0.07	0	0	0
C2	$NPV_{rel} \times 10^7$ [HKD]	2.45	2.57	2.57	2.57	2.57
	Difference %	4.49	0.05	0	0	0
C3	$NPV_{rel} \times 10^7$ [HKD]	2.41	2.53	2.53	2.53	2.53
	Difference %	4.68	0.14	0	0	0
C4	$NPV_{rel} \times 10^7$ [HKD]	2.31	2.38	2.38	2.38	2.38
	Difference %	3.06	0.09	0	0	0
C5	$NPV_{rel} \times 10^7$ [HKD]	2.28	2.33	2.33	2.33	2.33
	Difference %	2.25	0.05	0	0	0
C6	$NPV_{rel} \times 10^7$ [HKD]	2.23	2.26	2.26	2.26	2.26
	Difference %	1.43	0.03	0	0	0

5.2.4. Target investigation

In CLP's PDM programme, a mutually agreed target for energy demand reduction is specified, which the customer can attempt to achieve during the PDM event. While CLP encourages customers to reduce their energy demand beyond the target, they can only offer a maximum incentive payment for electricity demand reduction of up to 150% of the target for each event. This results in the value of the target being a significant factor in the PDM incentive and economic performance of the system. In a previous investigation, the target was assumed to be equal to the maximum energy demand value of the system during the entire year, which can be unrestricted when calculating the PDM incentive. Therefore, five different values of the target were assumed to explore the impact of the target on economic performance. These five different values of the target were 50, 100, 150, 200, and 250 kW. A battery capacity of 2000 kWh in S3 was selected for the target investigation. The NPV_{rel} results calculated from these five targets and the differences in NPV_{rel} from the original target are presented in Table 13. As can be observed from the data, when the target was greater than 150 kW, the NPV_{rel} results were consistent with the original target results. When the target was 100 kW, the differences in NPV_{rel} results were all within 0.2%. When the target was 50 kW, the variation in NPV_{rel} was less than 7%, with the largest difference being 6.61% in C1.

5.3. Investigation for tariff model and policy suggestion

Based on the results and discussions presented in Sections 5.2.2 and 5.2.3, positive NPV_{rel} results were only obtained when the hybrid ocean energy system was between 0% and 20% of its original scale in the absence of a feed-in tariff. This implied that without the feed-in tariff, which is a government subsidy for renewable energy, the economic viability of the studied zero-energy office building in Hong Kong was poor. Therefore, two possible approaches and suggestions for the refinement of the tariff model and PDM programme that can be used to promote renewable energy applications and improve the economic performance of systems with renewable energy generation were proposed and tested through TRNSYS simulations. The NPV_{rel} results are presented and discussed in this section. These two possible approaches for refinement are benchmark modifications and grid-exporting tariff modifications.

5.3.1. Investigation of Benchmark modifications

The first possible method for refinement is benchmark modifications of the PDM programme. In the original model framework, CLP defines the total reduction in electricity demand achieved by the customer by calculating the difference between the benchmark and actual electricity demand during the event period. This benchmark is defined as the average electricity demand in the same period of the relevant event of the three highest electricity demand days in the ten preceding non-event days. This benchmark is the normalised baseline mentioned in Section 3.3. This setup can result in several problems. First, flexibility control via the battery reduces the discharging line during the peak and reduces the benchmark. Second, when the hybrid ocean energy system consisting of 80% FPV systems is added to the all-grid case, the surplus energy, which is frequently present between 11 am and 3 pm, reduces both the benchmark and PDM incentives. These two problems affect the economic performance of the office building without the feed-in tariff and with the addition of a hybrid ocean renewable energy system. To improve the economic performance of the system and promote the economic viability of renewable energy without the feed-in tariff, we propose a new benchmark in response to the refinement of the original benchmark in S2 and S3. The original benchmark is called Benchmark 1 and the new benchmark is called Benchmark 2. Benchmark 2 is defined as the actual energy consumption of the office building in S1 for the same period of the event. A battery capacity of 200 kWh was selected from S2 and S3 for the benchmark modification investigation. The NPV_{rel} results for S2 in the Benchmark 1 and 2 cases are shown in Fig. 22, whereas the NPV_{rel} results for S3 are shown in Fig. 24. Based on the data in the tables and the NPV_{rel} variation curves in the figures, the NPV_{rel} results in both S2 and S3 exhibited a significant improvement after the addition of the hybrid ocean energy system when Benchmark 2 was applied, which proved the effectiveness of Benchmark 2. However, the NPV_{rel} results that were originally less than zero did not reach a neutral value.

As shown in Figs. 22 and 24, all the NPV_{rel} curves had two turning points at 30% and 60% of renewable energy generation. To investigate the reason for these two turning points, we selected C1 and C3 from scenarios 2 and 3, respectively, to decompose NPV_{rel} into the initial investment, annual cost, and annual income, respectively, as shown in Figs. 23 and 25. The curves for both annual cost and initial investment had a significant turning point at 30% of renewable energy generation, which resulted in the turning point of the NPV_{rel} curves at 30%. According to Table 13, from 10% to 30%, the main change in the hybrid ocean renewable energy system was the number of TSGs, whereas from 40% to 100%, the only increase was in the number of FPV modules. Comparing the FPV and TSG systems, the TSG system had a higher initial investment cost and a higher O&M cost, thus resulting in the turning point of the annual cost and initial investment curves at 30%. Meanwhile, the slope of the annual income curves decreased after 60%, meaning that the increase rate in annual income decreased when the percentage of renewable energy generation was greater than 60%, which resulted in another turning point in the NPV_{rel} curve at 60%.

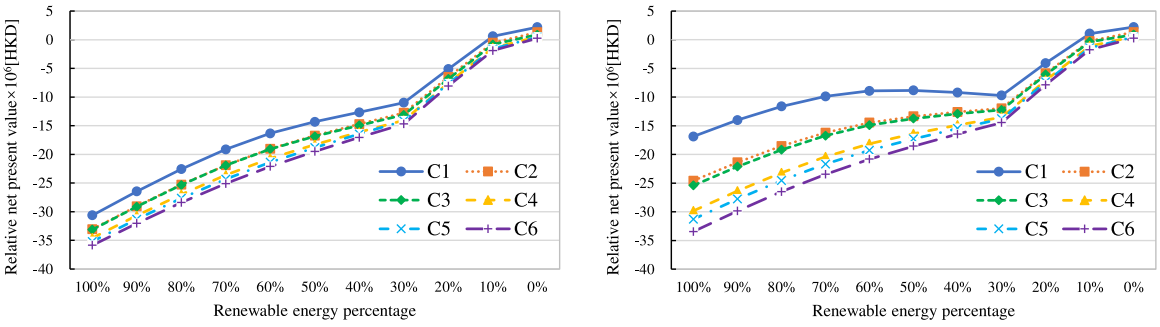

Fig. 22. NPV_{rel} curves of PDM cases in S2 with (a) Benchmark 1 and (b) Benchmark 2.

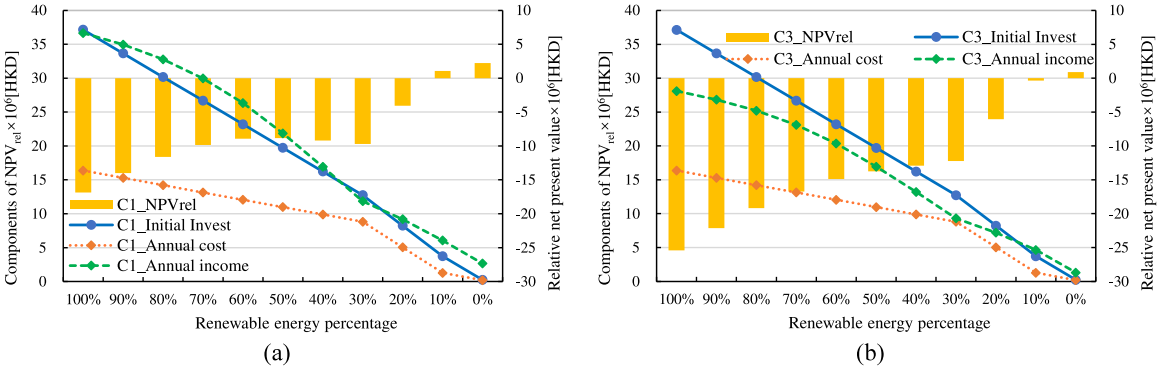

Fig. 23. Components of NPV_{rel} in (a) C1 and (b) C3 of S2.

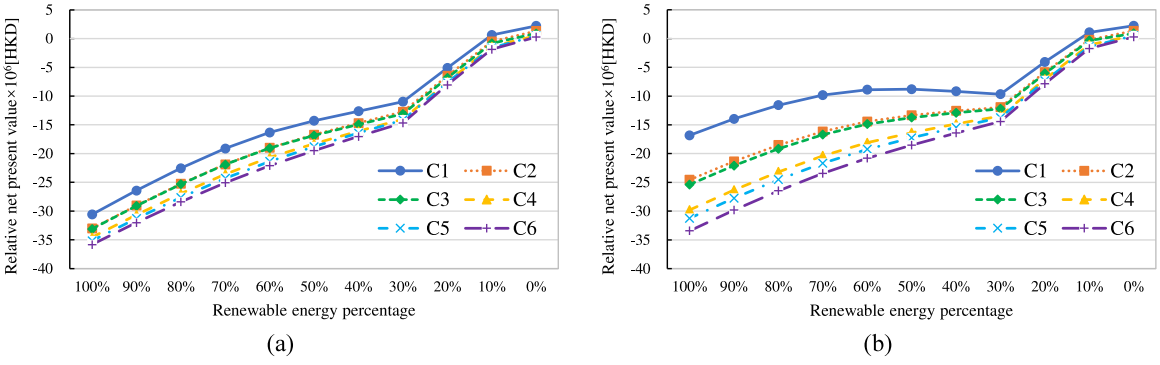

Fig. 24. NPV_{rel} curves of the PDM cases in S3 with (a) Benchmark 1 and (b) Benchmark 2.

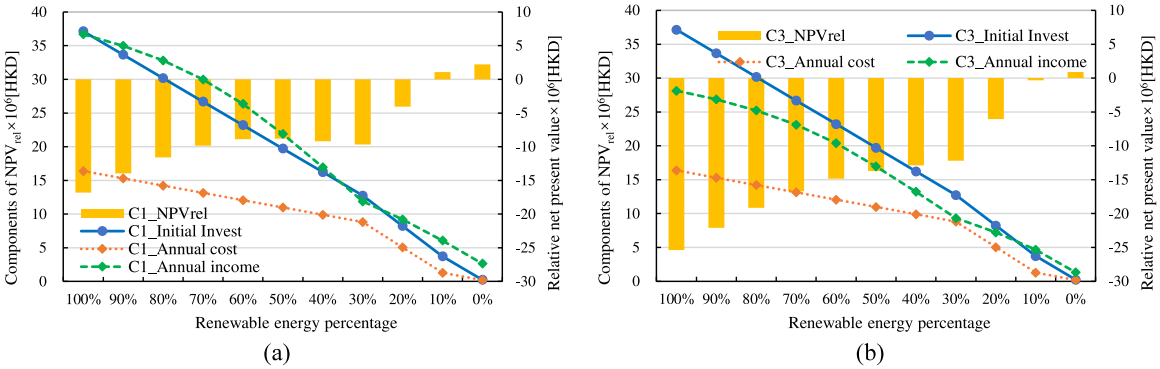

Fig. 25. Components of NPV_{rel} in (a) C1 and (b) C3 of S3.

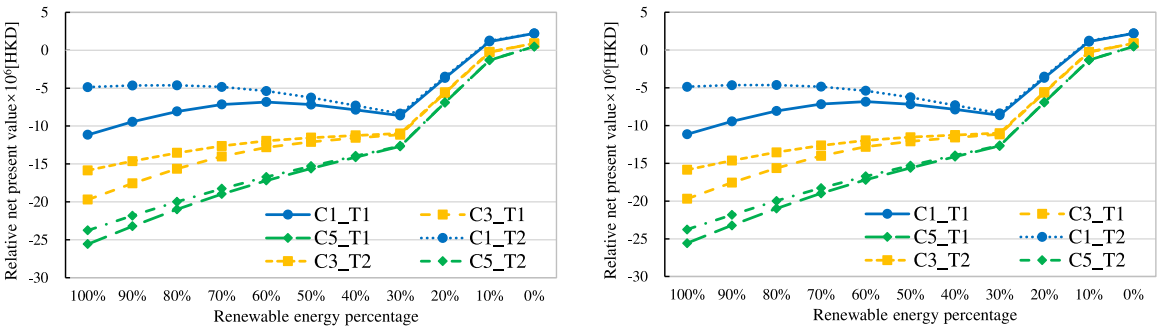

Fig. 26. NPV_{rel} curves of grid exporting tariffs T1 and T2 in (a) S2 (b) S3.

5.3.2. Investigation of energy exporting tariff and special energy exporting tariff during PDM events

After modifying the benchmark, we observed that although Benchmark 2 improved the economic performance of the system compared with Benchmark 1, it still failed to achieve a neutral NPV_{rel} value. Meanwhile, considering that exporting surplus renewable energy to the grid without the feed-in tariff does not provide any benefit to the system, two grid exporting tariffs are proposed to change this and further improve economic performance. The first grid exporting tariff was designated as T1. The parameter settings for T1 were derived from the commercial tariff model used in the system. During the peak period, the electricity export price was 0.737 HKD per kWh of exporting surplus energy, whereas, during the off-peak period, this value was 0.676 HKD per kWh. The electricity price escalation ratio was also considered in the grid exporting tariff year-by-year within a 20-year lifetime. The impact of the PDM programme was considered in the second grid exporting tariff T2. Only during the event period would the electric export price be 8 HKD per kWh, whereas, during the non-event period, the price would be the same as that of T1. Furthermore, the electricity price escalation ratio would not be added to this 8 HKD per kWh during the event period, and this value would remain consistent for a 20-year lifetime. C1, C3, and C5 from S2 and S3 with Benchmark 2 were selected for this investigation, and the NPV_{rel} results and curves are shown in Fig. 26.

The results of this investigation indicated that with the addition of grid exporting tariffs T1 and T2, the three cases selected from S2 and S3 demonstrated a significant improvement in economic performance compared with those without the grid exporting tariff. Meanwhile, when the percentage of renewable energy generation was greater than 30%, the NPV_{rel} value with T2 was higher than with T1 in the same case, and the magnitude of the difference was related to the frequency of the PDM event. However, the neutral NPV_{rel} values still occurred in the low percentage range of 0% to 20% without the feed-in tariff, and when the percentage of renewable energy generation increased, although the NPV_{rel} was significantly higher than those of cases without the grid exporting tariff, it still has difficulty in reaching a neutral value.

5.4. Sensitivity analysis

A sensitivity analysis was conducted to demonstrate the impact of different parameters on the economic performance of this hybrid system. In this system, two sensitive economic parameters which will affect the NPV_{rel} values were selected which were the interest rate and O&M percentage for both FPV and TSG system. Some cases with optimum economic performance from previous investigations were selected as examples to demonstrate the impact of interest rate and O&M percentage. For the interest rate investigation, a total of six cases were selected, which are the optimum economic performance cases in energy flexibility control and PDM control from S1, S2 and S3, named S1_FC, S1_PDM, S2_FC, S2_PDM, S3_FC, and S3_PDM respectively. For the O&M percentage investigation, as there were no ocean renewable energy systems in S1, the representative cases were S2_FC, S2_PDM, S3_FC, and S3_PDM. In S1_FC and S1_PDM, the battery capacity was 100 and 2000 kWh, and the battery capacities in S2_FC and S3_FC were 200 kWh, while in S2_PDM and S3_PDM, the batteries were both 50 kWh.

5.4.1. Interest rate

As part of the denominator in the NPV_{rel} formula, the variations in the interest rate will obviously affect the NPV_{rel} results. The original value of the interest rate was specified as 2.139% based on the five-year average value (2016–2020) of Hong Kong's real interest rate provided by the World Bank as described in the previous paragraph and used in the selected case G1C3. Therefore, in this interest rate sensitivity analysis, except the original value, the other values of interest rate were selected as 0%, 1%, 2%, 3%, 4%, 5% and 6%. The NPV_{rel} results of all the mentioned six cases with different interest rate values were shown in Fig. 27. As the magnitude of the NPV value of case S1_FC were much smaller than the other five cases, to show the trend, the results were shown separately in Fig. 27(a). The results from the original interest rate were marked with a red rounded rectangle. Based on these economic results, as the value of the interest rate increases, the NPV_{rel} results decreases, showing a significant downward trend. When the interest rate is less than the original value, larger NPV_{rel} results can be obtained for all cases, and when the interest rate was greater than the original value, smaller NPV_{rel} results were obtained for all cases. In case S1_FC, the result of NPV_{rel} became negative when the value of the interest rate was greater than or equal to 4%. In case S1_PDM, all the NPV_{rel} results were positive owing to the significant incentive gained by adding the PDM programme. Similarly, in the case with the ocean renewable energy systems, the NPV_{rel} values were all positive owing to the presence of the feed-in tariff. For every 1% decrease in interest rate, the NPV_{rel} value decreases by a different amount. It can be observed that the maximum decrease in NPV_{rel} for all six cases selected occurred when the interest rate increased from 0% to 1% and the minimum decrease occurred when the interest rate increased from 5% to 6%. The drop in NPV_{rel} value decreases as the interest rate increases. In case S1_FC, the minimum decrease in NPV_{rel} value was 8.12×10^3 HKD and the maximum decrease was 1.82×10^4 HKD. In case S1_PDM, the minimum decrease in NPV_{rel} value was 9.04×10^5 HKD and the maximum decrease was 1.82×10^5 HKD. In case S2_FC and S3_FC, the minimum decreases in NPV_{rel} value were about 3.79×10^6 HKD and the maximum

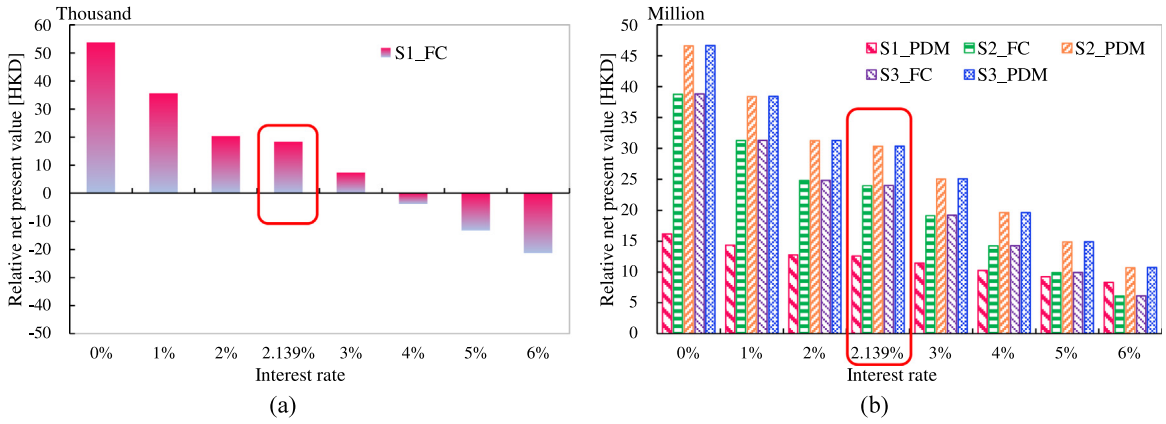

Fig. 27. NPV_{rel} results for (a) case S1_FC, (b) case S1_PDM, S2_FC, S2_PDM, S3_FC, and S3_PDM at different interest rates.

decreases were 7.50×10^6 and 7.51×10^6 HKD respectively. In case S2_PDM and S3_PDM, the minimum decreases in NPV_{rel} value were around 4.17×10^6 HKD and the maximum decreases were around 8.25×10^6 HKD.

5.4.2. O&M percentage

The annual O&M cost of the ocean renewable energy system is also an important parameter affecting the economic performance of the system, and changing the percentage used to calculate O&M costs can significantly affect the annual operating cost. In the original energy flexibility and PDM study, the O&M percentages for FPV and TSG system were 1.92% and 5% respectively. Therefore, in this sensitivity analysis, for FPV system, the O&M percentages were selected as 1%, 1.92%, 2%, 3% and 4%, while for TSG system, the O&M percentages were 2.5%, 5%, 7.5% and 10%. When the O&M percentages of one system varies, the O&M percentages of the other system remain the same to indicate the variation in NPV_{rel} results. In this O&M percentages sensitivity investigation, only the cases from the scenarios with hybrid renewable energy system were involved, which were S2_FC, S2_PDM, S3_FC, and S3_PDM. The NPV_{rel} results with different O&M percentages in FPV system was shown in Fig. 28(a), while the NPV_{rel} results with different O&M percentages in TSG system was shown in Fig. 28(b). Based on these results, the NPV_{rel} results were consistently reduced in all cases when the O&M percentage increases for both FPV and TSG systems. Meanwhile, whenever the O&M percentage of an FPV or TSG system increases, the NPV_{rel} values decreases significantly, but the value of the reduction may vary. When the O&M percentage of the FPV system increased, the reduction was consistent in all four cases. When the O&M percentage of FPV system increase from 1% to 2%, the drop of NPV_{rel} values was 4.41×10^6 HKD, when the O&M percentage increase from 2% to 3%, the drop of NPV_{rel} values was 4.77×10^6 HKD, and when O&M percentage increase from 3% to 4%, the drop of NPV_{rel} values was 8.83×10^6 HKD. However, for every 2.5% increase in the O&M percentage of the TSG system, the reduction in NPV_{rel} values was 3.85×10^6 HKD in all four cases. The NPV_{rel} results can be found to be more sensitive to changes in the O&M percentage of the FPV system compared to the TSG system. This is because the case G1C3 selected in this study was consisted by 2 TSG and 3967 FPV panels, with the FPV system accounting for 80% of the total. Therefore, the change in O&M percentage of the FPV system leads to a more significant change in NPV_{rel} value.

6. Conclusions

The implementation of renewable energy generation systems in buildings frequently results in a mismatch between building energy demand and instantaneous renewable energy generation. Owing to the pressure of electricity consumption, an increasing number of commercial electricity tariff models base their calculations on both demand and energy and distinguish between peak and off-peak periods. Because the calculation of the feed-in tariff in Hong Kong is based on renewable energy generation, a larger mismatch results in higher operational electricity costs, and no benefit is derived. Controlling energy use through the energy flexibility of the building can reduce this mismatch and further reduce the operational costs of the building. Meanwhile, to relieve pressure on the grid during peak periods, CLP proposed the PDM programme to encourage customers to shift or reduce their energy demand through an attractive incentive. Therefore, the impact of energy flexibility control and PDM programme was investigated in this study. Based on the existing tariff model and PDM programme two possible refinement suggestions were proposed, and their feasibility and validity were tested through simulations. Based on the simulation results, the following conclusions were drawn.

First, the impact of the energy flexibility control on the techno-economic performance of the entire system was investigated. Based on the basic principle of peak shaving and valley filling, two flexible control methods were designed by setting the same or different charging and discharging lines for each month, named FC1 and FC2, respectively. The battery capacity was the only variable. Based on the results, both flexibility control methods were effective in reducing operating costs. In scenario 1, the all-grid case, only positive NPV_{rel} values were obtained with the 100-kWh battery and the application of FC2; all other combinations obtained negative NPV_{rel} values. In contrast, in scenarios 2 and 3, positive NPV_{rel} values were obtained for all combinations owing to the presence of the feed-in tariff. Furthermore, the superior techno-economic performance indicated that FC2 was preferable for flexibility control. Because the energy demand varied from month to month throughout the year, the charging and discharging line in FC2, which was set according to the monthly energy demand, enabled better energy flexibility control to reduce the operational tariffs.

Second, the PDM programme proposed by CLP was applied to combinations using FC2 to explore the impact of PDM programme on the economic performance of the system. Similarly, two control methods were designed, called PDM Controls 1 and 2, for all three scenarios, where PDM Control 1 was consistent with the original FC2 and PDM Control 2 provided further control for PDM programme. The results of the simulations demonstrated that when the PDM programme was integrated into the tariff model, both PDM control methods resulted in a significant improvement in the economic performance of the studied system through the

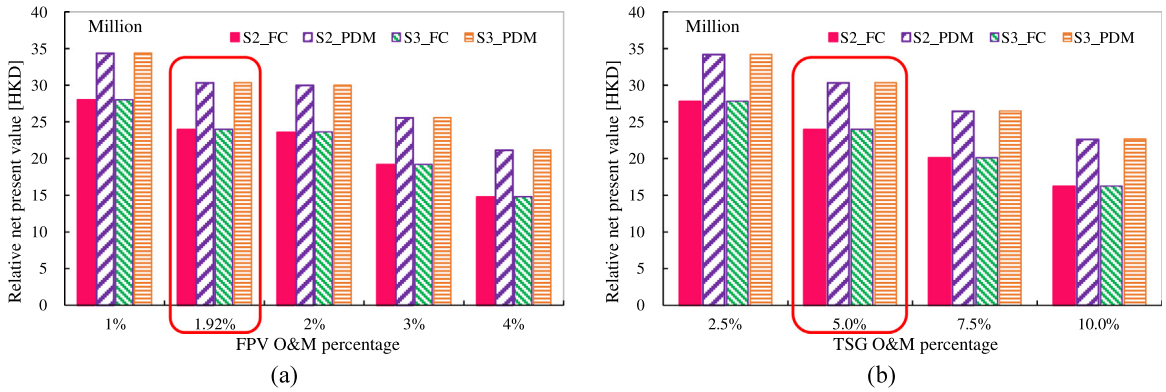

Fig. 28. NPV_{rel} results for selected cases at different O&M percentages of (a) FPV and (b) TSG systems.

incentives of the PDM programme. In S1, better economic performance was achieved with PDM Control 2 compared with PDM Control 1. In S2 and S3, the economic performances of cases with both PDM Controls 1 and 2 were similar when the battery capacity was small, and cases with PDM Control 2 obtained optimum economic performance when the battery capacity was larger. As participation in the PDM programme can provide an incentive to significantly improve economic performance, and the feed-in tariff is a government subsidy, in S2 and S3, we investigated what percentage of the original hybrid ocean renewable energy generation can achieve a neutral economic performance over a 20-year life cycle without the feed-in tariff. The results indicated that the maximum percentage of hybrid ocean energy systems that could achieve neutral NPV_{rel} values was between 20% and 30% of their original size. This demonstrated the low economic viability of applying full-scale renewable energy systems over a 20-year life cycle without a feed-in tariff. The impact of the PDM target on economic performance was also explored, with a non-significant maximum difference in NPV_{rel} of 6.61%.

Third, based on the previous results and performance, two possible suggestions were proposed for the refinement of the applied PDM programme and electricity tariff model to further increase the NPV_{rel} value and promote renewable energy. These two suggestions were benchmark modifications for the PDM programme and grid exporting tariff for the tariff model. The NPV_{rel} values obtained from the simulations of both proposals indicated significant improvements, proving the feasibility and effectiveness of both proposals. However, obtaining a positive economic performance when the percentage of renewable energy generation is above 30% is still difficult.

In summary, both energy flexibility control and the PDM programme can improve the economic performance of office buildings under the application of renewable energy systems. However, the economic viability of using a full-scale renewable energy generation system without a feed-in tariff is insufficient. To promote renewable energy, we propose benchmark modification and grid exporting tariffs to refine the existing electricity tariff model and the PDM programme. These two proposals can significantly improve economic performance; however, owing to the high investment and O&M costs of hybrid ocean energy systems and batteries, full-scale hybrid systems still cannot achieve neutral NPV_{rel} values. We consider that over time, when the investment costs of renewable energy systems and batteries decrease to a certain level, neutral economic performance can be achieved even without government subsidies such as feed-in tariffs.

The economic performance of the proposed hybrid system was observed to be improved with energy flexibility control and PDM programme in this study. Meanwhile, there are still several directions that could be investigated further in future research. Firstly, although energy flexibility control has been proved to improve economic performance, in the system studied, batteries are the only source of energy flexibility and require high investment costs. One of the future research directions will therefore focus on discovering energy storage capacity and sources of energy flexibility in renewable energy system itself to save the investment and improve the operational cost. Furthermore, a more sophisticated utility business model including grid exporting tariff will be another research point with the application of the PDM programme to encourage customers exporting renewable energy generation to the grid when it needed during the peak period. Finally, the application of energy flexibility and PDM programme to the community scale to uncover additional energy flexibility sources and further control and to investigate the performance will also be a focus of future research.

CRediT authorship contribution statement

Shijie Zhou: Methodology, Investigation, Writing – original draft, Writing – review & editing. **Sunliang Cao:** Supervision, Funding acquisition, Project administration, Conceptualization, Methodology, Investigation, Writing – original draft, Writing – review & editing.

Declaration of competing interest

The authors declare that they have no known competing financial interests or personal relationships that could have appeared to influence the work reported in this paper.

Data availability

Data will be made available on request.

Acknowledgements

This research is partially supported by the Project ID "P0033880" from Research Institute for Sustainable Urban Development (RISUD), Hong Kong Special Administrative Region, and partially supported by the Project ID "P0039664" from Research Institute for Smart Energy (RISE), The Hong Kong Polytechnic University.

Appendix A

See Table A.1.

Appendix B

See Table B.1.

Table A.1
NPV_{rel} results in S2 with different battery capacities and RE generation percentages under PDM Control 2.

Battery capacity [kWh]			200	400	600	800	1000	1200	1400	1600	1800	2000
C1: $NPV_{rel} \times 10^6$ [HKD]	G_{RE} percent [%]	100	−30.61	−30.92	−31.14	−31.27	−31.32	−31.29	−31.18	−31.38	−31.88	−32.51
		90	−26.45	−26.77	−26.97	−27.03	−27.01	−26.91	−26.65	−26.52	−26.88	−27.41
		80	−22.55	−22.88	−23.05	−23.03	−22.91	−22.71	−22.30	−21.81	−22.00	−22.52
		70	−19.12	−19.44	−19.56	−19.45	−19.21	−18.81	−18.21	−17.37	−17.23	−17.74
		60	−16.33	−16.63	−16.66	−16.42	−15.95	−15.33	−14.46	−13.42	−12.84	−13.16
		50	−14.30	−14.57	−14.44	−13.94	−13.22	−12.28	−11.17	−9.91	−8.98	−8.97
		40	−12.64	−12.79	−12.34	−11.53	−10.47	−9.31	−8.14	−6.92	−5.75	−5.52
		30	−10.98	−10.75	−9.91	−8.84	−7.82	−6.79	−5.79	−4.62	−3.40	−2.84
		20	−5.10	−4.85	−3.86	−2.61	−1.30	−0.12	1.08	2.30	3.58	4.39
		10	0.62	0.99	2.15	3.57	4.87	6.14	7.36	8.58	9.84	10.85
		0	2.22	3.32	4.47	5.57	6.60	7.76	8.94	10.15	11.39	12.58
C2: $NPV_{rel} \times 10^6$ [HKD]	G_{RE} percent [%]	100	−33.04	−33.34	−33.57	−33.74	−33.89	−34.00	−34.10	−34.31	−34.73	−35.25
		90	−29.04	−29.34	−29.56	−29.70	−29.80	−29.87	−29.87	−29.89	−30.24	−30.70
		80	−25.27	−25.58	−25.78	−25.87	−25.91	−25.93	−25.83	−25.65	−25.88	−26.33
		70	−21.89	−22.19	−22.37	−22.40	−22.37	−22.27	−22.05	−21.67	−21.69	−22.13
		60	−19.01	−19.31	−19.43	−19.39	−19.22	−18.98	−18.59	−18.09	−17.85	−18.17
		50	−16.72	−16.99	−17.02	−16.82	−16.51	−16.07	−15.52	−14.89	−14.45	−14.56
		40	−14.71	−14.91	−14.74	−14.37	−13.85	−13.26	−12.70	−12.11	−11.54	−11.55
		30	−12.73	−12.70	−12.30	−11.77	−11.32	−10.86	−10.44	−9.89	−9.29	−9.07
		20	−6.48	−6.43	−5.92	−5.30	−4.63	−4.08	−3.51	−2.93	−2.30	−1.95
		10	−0.50	−0.37	0.22	0.96	1.59	2.21	2.79	3.36	3.97	4.43
		0	1.33	1.92	2.41	2.90	3.34	3.89	4.44	5.03	5.62	6.20
C3: $NPV_{rel} \times 10^6$ [HKD]	G_{RE} percent [%]	100	−33.13	−33.44	−33.70	−33.88	−34.08	−34.21	−34.32	−34.63	−35.07	−35.49
		90	−29.12	−29.43	−29.68	−29.84	−30.01	−30.10	−30.13	−30.28	−30.65	−31.02
		80	−25.33	−25.64	−25.88	−26.00	−26.13	−26.16	−26.10	−26.07	−26.40	−26.75
		70	−21.91	−22.22	−22.43	−22.52	−22.57	−22.51	−22.38	−22.16	−22.31	−22.67
		60	−19.06	−19.36	−19.52	−19.55	−19.49	−19.33	−19.05	−18.68	−18.56	−18.90
		50	−16.86	−17.15	−17.23	−17.16	−16.93	−16.59	−16.18	−15.69	−15.34	−15.51
		40	−14.93	−15.17	−15.12	−14.81	−14.37	−13.90	−13.42	−12.93	−12.48	−12.44
		30	−13.11	−13.17	−12.81	−12.32	−11.86	−11.44	−11.02	−10.61	−10.14	−9.90
		20	−6.83	−6.86	−6.46	−5.86	−5.31	−4.76	−4.23	−3.70	−3.17	−2.83
		10	−0.82	−0.76	−0.27	0.37	0.99	1.56	2.11	2.64	3.17	3.58
		0	0.89	1.44	2.05	2.54	2.91	3.39	3.85	4.32	4.79	5.23
C4: $NPV_{rel} \times 10^6$ [HKD]	G_{RE} percent [%]	100	−34.59	−34.88	−35.14	−35.34	−35.60	−35.81	−36.03	−36.32	−36.71	−37.06
		90	−30.68	−30.98	−31.23	−31.43	−31.66	−31.84	−32.01	−32.23	−32.57	−32.90
		80	−26.97	−27.28	−27.53	−27.70	−27.91	−28.06	−28.16	−28.28	−28.61	−28.91
		70	−23.60	−23.90	−24.13	−24.29	−24.46	−24.55	−24.61	−24.61	−24.84	−25.16
		60	−20.69	−20.98	−21.18	−21.31	−21.40	−21.44	−21.41	−21.32	−21.38	−21.71
		50	−18.29	−18.57	−18.73	−18.81	−18.79	−18.72	−18.60	−18.44	−18.37	−18.60
		40	−16.11	−16.36	−16.45	−16.38	−16.23	−16.08	−15.93	−15.76	−15.64	−15.74
		30	−14.04	−14.18	−14.08	−13.90	−13.75	−13.64	−13.54	−13.44	−13.31	−13.28
		20	−7.54	−7.65	−7.53	−7.29	−7.08	−6.89	−6.69	−6.51	−6.33	−6.27
		10	−1.38	−1.45	−1.27	−1.02	−0.76	−0.55	−0.36	−0.17	0.01	0.12
		0	0.52	0.76	0.97	1.11	1.16	1.31	1.43	1.56	1.69	1.80
C5: $NPV_{rel} \times 10^6$ [HKD]	G_{RE} percent [%]	100	−35.19	−35.48	−35.72	−35.94	−36.13	−36.32	−36.46	−36.76	−37.14	−37.59
		90	−31.32	−31.60	−31.85	−32.06	−32.23	−32.40	−32.50	−32.72	−33.09	−33.53
		80	−27.65	−27.93	−28.18	−28.38	−28.52	−28.65	−28.72	−28.84	−29.19	−29.63
		70	−24.32	−24.60	−24.84	−25.02	−25.11	−25.19	−25.23	−25.25	−25.51	−25.94
		60	−21.37	−21.65	−21.88	−22.01	−22.04	−22.07	−22.04	−21.99	−22.11	−22.52
		50	−18.81	−19.08	−19.26	−19.33	−19.28	−19.24	−19.19	−19.12	−19.14	−19.48
		40	−16.44	−16.68	−16.77	−16.72	−16.61	−16.58	−16.54	−16.48	−16.45	−16.70
		30	−14.15	−14.31	−14.25	−14.18	−14.13	−14.12	−14.10	−14.11	−14.05	−14.17
		20	−7.67	−7.79	−7.70	−7.57	−7.46	−7.37	−7.28	−7.19	−7.10	−7.18
		10	−1.59	−1.66	−1.50	−1.31	−1.12	−1.02	−0.94	−0.86	−0.75	−0.76
		0	0.49	0.65	0.80	0.80	0.72	0.77	0.82	0.87	0.91	0.94
C6: $NPV_{rel} \times 10^6$ [HKD]	G_{RE} percent [%]	100	−35.86	−36.14	−36.39	−36.62	−36.83	−37.07	−37.28	−37.58	−37.94	−38.35
		90	−32.03	−32.31	−32.57	−32.79	−32.99	−33.22	−33.41	−33.66	−34.03	−34.45
		80	−28.40	−28.69	−28.94	−29.16	−29.35	−29.55	−29.73	−29.92	−30.27	−30.69
		70	−25.08	−25.36	−25.62	−25.83	−25.99	−26.17	−26.32	−26.46	−26.74	−27.16
		60	−22.11	−22.39	−22.64	−22.83	−22.95	−23.09	−23.21	−23.31	−23.51	−23.90
		50	−19.49	−19.76	−19.98	−20.13	−20.21	−20.31	−20.42	−20.52	−20.66	−21.01
		40	−17.04	−17.29	−17.46	−17.54	−17.58	−17.72	−17.82	−17.93	−18.04	−18.33
		30	−14.68	−14.89	−14.95	−15.04	−15.13	−15.26	−15.39	−15.55	−15.65	−15.84
		20	−8.05	−8.23	−8.29	−8.33	−8.38	−8.46	−8.54	−8.62	−8.70	−8.90
		10	−1.86	−2.00	−2.02	−2.02	−2.02	−2.10	−2.19	−2.28	−2.36	−2.50
		0	0.27	0.28	0.24	0.07	−0.16	−0.29	−0.41	−0.53	−0.66	−0.79

Table B.1
NPV_{rel} results in S3 with different battery capacities and RE generation percentages under PDM Control 2.

Battery capacity [kWh]			200	400	600	800	1000	1200	1400	1600	1800	2000
C1: $NPV_{rel} \times 10^6$ [HKD]	G_{RE} percent [%]	100	−30.58	−30.89	−31.09	−31.19	−31.21	−31.15	−31.02	−31.39	−31.87	−32.40
		90	−26.43	−26.74	−26.92	−26.96	−26.90	−26.78	−26.50	−26.55	−27.01	−27.56
		80	−22.53	−22.84	−22.99	−22.96	−22.81	−22.58	−22.13	−21.75	−22.15	−22.68
		70	−19.10	−19.40	−19.50	−19.38	−19.11	−18.68	−18.04	−17.21	−17.36	−17.90
		60	−16.31	−16.59	−16.61	−16.35	−15.84	−15.19	−14.29	−13.18	−12.85	−13.32
		50	−14.29	−14.52	−14.38	−13.86	−13.11	−12.15	−11.01	−9.70	−8.91	−9.25
		40	−12.63	−12.73	−12.28	−11.44	−10.35	−9.17	−7.96	−6.73	−5.66	−5.65
		30	−10.96	−10.70	−9.84	−8.74	−7.72	−6.67	−5.65	−4.47	−3.27	−2.81
		20	−5.10	−4.84	−3.83	−2.59	−1.28	−0.10	1.07	2.27	3.53	4.30
		10	0.63	1.00	2.15	3.57	4.87	6.13	7.34	8.56	9.82	10.80
		0	2.22	3.32	4.47	5.57	6.60	7.76	8.94	10.15	11.39	12.58
C2: $NPV_{rel} \times 10^6$ [HKD]	G_{RE} percent [%]	100	−33.01	−33.30	−33.51	−33.66	−33.77	−33.85	−33.92	−34.22	−34.61	−35.07
		90	−29.01	−29.31	−29.51	−29.62	−29.69	−29.73	−29.71	−29.83	−30.19	−30.66
		80	−25.25	−25.54	−25.73	−25.80	−25.81	−25.80	−25.66	−25.53	−25.86	−26.32
		70	−21.87	−22.15	−22.31	−22.33	−22.27	−22.15	−21.89	−21.49	−21.66	−22.12
		60	−18.99	−19.26	−19.38	−19.31	−19.12	−18.85	−18.43	−17.87	−17.78	−18.17
		50	−16.70	−16.94	−16.96	−16.74	−16.41	−15.94	−15.37	−14.70	−14.35	−14.67
		40	−14.69	−14.85	−14.68	−14.28	−13.73	−13.13	−12.53	−11.93	−11.42	−11.55
		30	−12.71	−12.65	−12.23	−11.67	−11.21	−10.73	−10.29	−9.73	−9.16	−8.99
		20	−6.47	−6.42	−5.91	−5.28	−4.61	−4.06	−3.51	−2.96	−2.36	−2.01
		10	−0.50	−0.37	0.22	0.97	1.59	2.21	2.77	3.35	3.95	4.39
		0	1.33	1.92	2.41	2.90	3.34	3.89	4.44	5.03	5.62	6.20
C3: $NPV_{rel} \times 10^6$ [HKD]	G_{RE} percent [%]	100	−33.10	−33.40	−33.64	−33.80	−33.98	−34.10	−34.17	−34.56	−35.00	−35.43
		90	−29.10	−29.40	−29.63	−29.77	−29.92	−29.99	−29.97	−30.22	−30.66	−31.09
		80	−25.31	−25.61	−25.83	−25.93	−26.04	−26.05	−25.96	−25.98	−26.42	−26.84
		70	−21.90	−22.19	−22.38	−22.46	−22.49	−22.41	−22.23	−22.00	−22.34	−22.76
		60	−19.04	−19.32	−19.48	−19.49	−19.40	−19.23	−18.90	−18.49	−18.52	−18.97
		50	−16.85	−17.10	−17.19	−17.09	−16.84	−16.48	−16.03	−15.50	−15.17	−15.54
		40	−14.92	−15.12	−15.07	−14.74	−14.28	−13.78	−13.27	−12.74	−12.31	−12.42
		30	−13.10	−13.14	−12.75	−12.23	−11.76	−11.31	−10.89	−10.45	−9.96	−9.77
		20	−6.82	−6.85	−6.44	−5.84	−5.29	−4.74	−4.20	−3.67	−3.13	−2.81
		10	−0.81	−0.76	−0.26	0.36	1.00	1.56	2.11	2.64	3.17	3.56
		0	0.89	1.44	2.05	2.54	2.91	3.39	3.85	4.32	4.79	5.23
C4: $NPV_{rel} \times 10^6$ [HKD]	G_{RE} percent [%]	100	−34.56	−34.85	−35.08	−35.26	−35.50	−35.70	−35.86	−36.20	−36.57	−36.95
		90	−30.65	−30.94	−31.18	−31.35	−31.57	−31.73	−31.85	−32.10	−32.48	−32.85
		80	−26.95	−27.24	−27.48	−27.63	−27.82	−27.95	−28.02	−28.15	−28.53	−28.89
		70	−23.58	−23.87	−24.08	−24.23	−24.37	−24.45	−24.45	−24.44	−24.77	−25.13
		60	−20.67	−20.94	−21.14	−21.25	−21.32	−21.34	−21.26	−21.13	−21.27	−21.67
		50	−18.27	−18.52	−18.69	−18.74	−18.70	−18.61	−18.46	−18.25	−18.18	−18.53
		40	−16.10	−16.31	−16.41	−16.31	−16.15	−15.96	−15.78	−15.58	−15.44	−15.63
		30	−14.02	−14.15	−14.03	−13.82	−13.65	−13.51	−13.40	−13.28	−13.12	−13.13
		20	−7.53	−7.65	−7.52	−7.27	−7.07	−6.86	−6.67	−6.48	−6.29	−6.24
		10	−1.38	−1.45	−1.26	−1.02	−0.76	−0.55	−0.36	−0.17	0.01	0.10
		0	0.52	0.76	0.97	1.11	1.16	1.31	1.43	1.56	1.69	1.80
C5: $NPV_{rel} \times 10^6$ [HKD]	G_{RE} percent [%]	100	−35.16	−35.44	−35.67	−35.86	−36.02	−36.19	−36.29	−36.61	−36.98	−37.42
		90	−31.29	−31.57	−31.80	−31.98	−32.13	−32.27	−32.33	−32.58	−32.96	−33.40
		80	−27.62	−27.90	−28.14	−28.31	−28.42	−28.53	−28.56	−28.71	−29.08	−29.52
		70	−24.29	−24.57	−24.79	−24.95	−25.02	−25.08	−25.08	−25.09	−25.41	−25.86
		60	−21.35	−21.61	−21.83	−21.95	−21.95	−21.96	−21.90	−21.82	−22.05	−22.51
		50	−18.80	−19.04	−19.22	−19.27	−19.19	−19.13	−19.05	−18.98	−19.04	−19.46
		40	−16.42	−16.64	−16.73	−16.66	−16.51	−16.47	−16.40	−16.32	−16.32	−16.62
		30	−14.14	−14.27	−14.19	−14.11	−14.03	−13.99	−13.99	−13.98	−13.93	−14.07
		20	−7.66	−7.79	−7.69	−7.56	−7.44	−7.35	−7.25	−7.16	−7.07	−7.18
		10	−1.59	−1.65	−1.50	−1.31	−1.12	−1.02	−0.94	−0.85	−0.76	−0.78
		0	0.49	0.65	0.80	0.80	0.72	0.77	0.82	0.87	0.91	0.94
C6: $NPV_{rel} \times 10^6$ [HKD]	G_{RE} percent [%]	100	−35.83	−36.10	−36.33	−36.53	−36.71	−36.93	−37.10	−37.40	−37.74	−38.15
		90	−32.00	−32.28	−32.51	−32.72	−32.89	−33.10	−33.24	−33.50	−33.84	−34.25
		80	−28.38	−28.65	−28.89	−29.09	−29.25	−29.44	−29.56	−29.77	−30.10	−30.51
		70	−25.06	−25.33	−25.57	−25.77	−25.90	−26.05	−26.17	−26.29	−26.59	−27.00
		60	−22.09	−22.35	−22.59	−22.76	−22.86	−22.98	−23.06	−23.14	−23.41	−23.83
		50	−19.47	−19.72	−19.94	−20.07	−20.12	−20.21	−20.28	−20.38	−20.53	−20.93
		40	−17.02	−17.25	−17.42	−17.48	−17.49	−17.60	−17.68	−17.77	−17.88	−18.20
		30	−14.66	−14.85	−14.90	−14.96	−15.02	−15.13	−15.27	−15.42	−15.52	−15.72
		20	−8.05	−8.23	−8.28	−8.31	−8.36	−8.44	−8.51	−8.59	−8.67	−8.88
		10	−1.86	−2.00	−2.01	−2.02	−2.02	−2.10	−2.19	−2.28	−2.37	−2.51
		0	0.27	0.28	0.24	0.07	−0.16	−0.29	−0.41	−0.53	−0.66	−0.79

References

Anzar, M., Iqra, R., Kousar, A., Ejaz, S., Alvarez-Alvarado, M.S., Zafar, A.K., 2017. Optimization of home energy management system in smart grid for effective demand side management. In: 2017 International Renewable and Sustainable Energy Conference. IRSEC.

Bhattacharya, S., Chengoden, R., Srivastava, G., Alazab, M., Javed, A.R., Victor, N., Maddikunta, P.K., Gadekallu, T.R., 2022. Incentive mechanisms for smart grid: State of the art, challenges, open issues, future directions. Big Data Cogn. Comput. 6 (2), http://dx.doi.org/10.3390/bdcc6020047.

Cao, S., 2019. The impact of electric vehicles and mobile boundary expansions on the realization of zero-emission office buildings. Appl. Energy 251, 113347. http://dx.doi.org/10.1016/j.apenergy.2019.113347.

Cazzaniga, R., Rosa-Clot, M., 2021. The booming of floating PV. Sol. Energy 219, 3–10. http://dx.doi.org/10.1016/j.solener.2020.09.057.
Census and Statistics Department, 2022. Hong Kong energy statistics annual report. https://www.censtatd.gov.hk/en/EIndexbySubject.html?pcode=B1100002&scode=90.
Chen, F., 2013. The Kuroshio Power Plant. Vol. 225. Springer, http://dx.doi.org/10.1007/978-3-319-00822-6.
Chiang, C.-H., Young, C.-H., 2022. An engineering project for a flood detention pond surface-type floating photovoltaic power generation system with an installed capacity of 32,600.88 KWp. Energy Rep. 8, 2219–2232. http://dx.doi.org/10.1016/j.egyr.2022.01.156.
CLP, 2021a. CLP 2021 electricity tariff tables: Bulk tariff. https://www.clp.com.hk/content/dam/clphk/documents/customer-service-site/tariff-site/Tariff%20Table-English%20(2021-01-01).pdf.
CLP, 2021b. Peak demand management. https://www.clp.com.hk/en/environment/funds-services/peak-demand-management.html.
CLP, 2022. Feed-in tariff (residential)-benefits. https://www.clp.com.hk/en/residential/low-carbon-living/feed-in-tariff-residential/benefits.
CNBC, 2021. G-20 leaders struggle to secure climate breakthrough at Rome summit. https://www.cnbc.com/2021/10/31/g-20-leaders-struggle-to-secure-climate-breakthrough-at-rome-summit-.html.
Coles, D., Angeloudis, A., Goss, Z., Miles, J., 2021. Tidal stream vs wind energy: the value of cyclic power when combined with short-term storage in hybrid systems. Energies 14 (4), 1106, https://www.mdpi.com/1996-1073/14/4/1106.
Dar, U.I., Sartori, I., Georges, L., Novakovic, V., 2014. Advanced control of heat pumps for improved flexibility of net-ZEB towards the grid. Energy Build. 69, 74–84. http://dx.doi.org/10.1016/j.enbuild.2013.10.019.
Elahee, K., Jugoo, S., 2013. Ocean thermal energy for air-conditioning: Case study of a green data center. Energy Sources A Recov. Util. Environ. Eff. 35 (7), 679–684. http://dx.doi.org/10.1080/15567036.2010.504941.
Electrical & Mechanical Services Department (EMSD), 2007. Performance-based building energy code. https://www.emsd.gov.hk/filemanager/en/content_724/pb-bec_2007.pdf.
EnergyPlan, 2021. TRNSYS. https://www.energyplan.eu/othertools/local/trnsys/.
Environmental Protection Department (EPD), 2005. Marine quality introduction. https://www.epd.gov.hk/epd/misc/marine_quality/1986-2005/eng/introduction_content.htm.
Faria, P., Vale, Z., 2022. Application of distinct demand response program during the ramping and sustained response period. Energy Rep. 8, 411–416. http://dx.doi.org/10.1016/j.egyr.2022.01.044.
Finck, C., Li, R., Kramer, R., Zeiler, W., 2018. Quantifying demand flexibility of power-to-heat and thermal energy storage in the control of building heating systems. Appl. Energy 209, 409–425. http://dx.doi.org/10.1016/j.apenergy.2017.11.036.
Fraenkel, P.L., 2002. Power from marine currents. Proc. Inst. Mech. Eng. A J. Power Energy 216 (1), 1–14. http://dx.doi.org/10.1243/095765002760024782.
Fraenkel, P.L., 2006. Tidal current energy technologies. Ibis 148 (s1), 145–151. http://dx.doi.org/10.1111/j.1474-919X.2006.00518.x.
FuturaSun, 2017. FU 250/ 255/ 260/ 265/ 270/ 275 P polycrystalline photovoltaic module - 60 cells. http://www.futurasun.com/wp-content/uploads/2018/01/2017_HK60p_250-275_4busbar_en_v3.pdf?x97762.
Ghasempour, A., 2016. Optimum number of aggregators based on power consumption, cost, and network lifetime in advanced metering infrastructure architecture for smart grid internet of things.
Ghasempour, A., 2017. Advanced metering infrastructure in smart grid: Requirements, challenges, architectures, technologies, and optimizations. pp. 77–127.
Ghasempour, A., 2019. Internet of things in smart grid: Architecture, applications, services, key technologies, and challenges. Inventions 4 (22), http://dx.doi.org/10.3390/inventions4010022.
Greentechmedia, 2019. Floating solar gets ready for the high seas. https://www.greentechmedia.com/articles/read/floating-solar-gears-up-for-the-high-seas.
Guo, X., Cao, S., Xu, Y., Zhu, X., 2021. The feasibility of using zero-emission electric boats to enhance the techno-economic performance of an ocean-energy-Supported Coastal hotel building. Energies 14 (24), 8465, https://www.mdpi.com/1996-1073/14/24/8465.
Hardisty, J., 2012. The tidal stream power curve: a case study. Energy Power Eng. 4 (3), 132–136.
Hong Kong Green Building Council (HKGBC), 2016. Hong Kong green office guide. https://www.hkgbc.org.hk/eng/gog.aspx.
Hsieh, I.Y.L., Pan, M.S., Chiang, Y.-M., Green, W.H., 2019. Learning only buys you so much: Practical limits on battery price reduction. Appl. Energy 239, 218–224. http://dx.doi.org/10.1016/j.apenergy.2019.01.138.
Huang, W., Zhang, N., Kang, C., Li, M., Huo, M., 2019. From demand response to integrated demand response: review and prospect of research and application. Prot. Control Mod. Power Syst. 4 (1), 12. http://dx.doi.org/10.1186/s41601-019-0126-4.
Hydrographic office (HKHO), 2017. Hong Kong tidal stream prediction system. https://current.hydro.gov.hk/en/map.html.
IEA, 2021. IEA EBC - annex 82 - energy flexible buildings towards resilient low carbon energy systems. https://annex82.iea-ebc.org/.
Intelligentliving, 2021. Commercial-scale floating solar projects in open seas under development. https://www.intelligentliving.co/commercial-scale-floating-solar-projects/.
Irshad, Z., Aejaz, S.M.H., Mustafa, U., Durrani, A.M.F., Hafeez, F., 2020. User-friendly demand side management for smart grid network. In: 2020 International Conference on Engineering and Emerging Technologies. ICEET.
Javaid, N., Hafeez, G., Iqbal, S., Alrajeh, N., Alabed, M.S., Guizani, M., 2018. Energy efficient integration of renewable energy sources in the smart grid for demand side management. IEEE Access 6, 77077–77096. http://dx.doi.org/10.1109/ACCESS.2018.2866461.
Kirkerud, J.G., Nagel, N.O., Bolkesjø, T.F., 2021. The role of demand response in the future renewable northern European energy system. Energy 235, 121336. http://dx.doi.org/10.1016/j.energy.2021.121336.
Kumar, M., Niyaz, H. Mohammed, Gupta, R., 2021. Challenges and opportunities towards the development of floating photovoltaic systems. Sol. Energy Mater. Sol. Cells 233, 111408. http://dx.doi.org/10.1016/j.solmat.2021.111408.
Lands Department (LandsD), 2020. Hong Kong geographic data (include area by district council). https://www.landsd.gov.hk/en/resources/mapping-information/hk-geographic-data.html.
Liu, M., Heiselberg, P., 2019. Energy flexibility of a nearly zero-energy building with weather predictive control on a convective building energy system and evaluated with different metrics. Appl. Energy 233-234, 764–775. http://dx.doi.org/10.1016/j.apenergy.2018.10.070.
Lou, J., 2017. Smart Grids: Emerging Technologies, Challenges and Future Directions. Nova Science Publishers.
Lu, F., Yu, Z., Zou, Y., Yang, X., 2021. Cooling system energy flexibility of a nearly zero-energy office building using building thermal mass: Potential evaluation and parametric analysis. Energy Build. 236, 110763. http://dx.doi.org/10.1016/j.enbuild.2021.110763.
Luo, H., Cao, S., Lu, V.L., 2022. The techno-economic feasibility of a coastal zero-energy hotel building supported by the hybrid wind–wave energy system. Sustain. Energy Grids Netw. 30, 100650. http://dx.doi.org/10.1016/j.segan.2022.100650.
MeteotestAG, 2021. Meteonorm. https://meteonorm.com/en/.
Mokhtari, R., Arabkoohsar, A., 2021. Feasibility study and multi-objective optimization of seawater cooling systems for data centers: A case study of Caspian Sea. Sustain. Energy Technol. Assess. 47, 101528. http://dx.doi.org/10.1016/j.seta.2021.101528.
NREL, 2021. Cost of renewable energy. https://www.nrel.gov/analysis/tech-lcoe-re-cost-est.html.
Oceansofenergy, 2020. Oceans of energy north sea. https://oceansofenergy.blue/north-sea-1/.
Paixão Martins, B., 2019. Techno-economic evaluation of a floating PV system for a wastewater treatment facility.
Park, E.S., Lee, T.S., 2021. The rebirth and eco-friendly energy production of an artificial lake: A case study on the tidal power in South Korea. Energy Rep. 7, 4681–4696. http://dx.doi.org/10.1016/j.egyr.2021.07.006.
Salpakari, J., Lund, P., 2016. Optimal and rule-based control strategies for energy flexibility in buildings with PV. Appl. Energy 161, 425–436. http://dx.doi.org/10.1016/j.apenergy.2015.10.036.
Selvakkumaran, S., Eriksson, L., Svensson, I.-L., 2021. How do business models for prosumers in the district energy sector capture flexibility? Energy Rep. 7, 203–212. http://dx.doi.org/10.1016/j.egyr.2021.08.154.
Solar Energy Laboratory (SEL), 2017. The University of Wisconsin-Madison. TRANSSOLAR energietechnik GmbH, CSTB – centre scientifique et technique du Bâtiment, TESS – thermal energy systems specialists. Section 8.7 meteonorm data. Volume 8 weather data. TRNSYS 18 document package.
SolarEdition, 2020. The FIRST UAE offshore open sea floating solar power plant is powering up soon. https://solaredition.com/the-first-uae-offshore-open-sea-floating-solar-power-plant-is-powering-up-soon/.
Soliman, M.S., Belkhier, Y., Ullah, N., Achour, A., Alharbi, Y.M., Al Alahmadi, A.A., Abeida, H., Khraisat, Y.S.H., 2021. Supervisory energy management of a hybrid battery/PV/tidal/wind sources integrated in DC-microgrid energy storage system. Energy Rep. 7, 7728–7740. http://dx.doi.org/10.1016/j.egyr.2021.11.056.
Statkraft, 2019. Statkraft selects norwegian ocean sun to supply floating solar plant in Albania. https://www.statkraft.com/newsroom/news-and-stories/archive/2019/floating-solar-pv/.
The University of Wisconsin Madison (UW-Madison), 2021. TRNSYS – official website. https://sel.me.wisc.edu/trnsys/features/features.html.
Tostado-Véliz, M., Arévalo, P., Kamel, S., Zawbaa, H.M., Jurado, F., 2022. Home energy management system considering effective demand response strategies and uncertainties. Energy Rep. 8, 5256–5271. http://dx.doi.org/10.1016/j.egyr.2022.04.006.
World Bank, 2021a. Real interest rate (%) - Hong Kong SAR, China. https://data.worldbank.org/indicator/FR.INR.RINR?end=2019&locations=HK&start=2010&view=chart.
World Bank, 2021b. Official exchange rate (LCU per US$, period average) - Hong Kong SAR, China. https://data.worldbank.org/indicator/PA.NUS.FCRF?end=2019&locations=HK&start=2011.

Zhou, Y., Cao, S., 2019. Energy flexibility investigation of advanced grid-responsive energy control strategies with the static battery and electric vehicles: A case study of a high-rise office building in Hong Kong. Energy Convers. Manage. 199, 111888. http://dx.doi.org/10.1016/j.enconman.2019.111888.

Zhou, S., Cao, S., Wang, S., 2022. Realisation of a coastal zero-emission office building with the support of hybrid ocean thermal, floating photovoltaics, and tidal stream generators. Energy Convers. Manage. 253, 115135. http://dx.doi.org/10.1016/j.enconman.2021.115135.